

Carbon Cloth Phenolic Composites For  
Ablative Rocket Nozzle Liners

# Phenolic Resin Chemistry and Proposed Mechanism for Thermal Decomposition

*Randy Lee*

July 2007

Jacobs Technology

*NASA Marshall Space Flight Center*

Non Metallic Materials and Processes Branch  
Ceramics & Ablatives Engineering



## Introduction & Preface

Phenolic matrix composites are often used in applications requiring advanced performance capabilities such as high temperature resistance, ablative protection and high carbonization yield in which most of the more traditional resins are quite deficient. Because of their high carbonaceous content and extensive crosslinked network, phenolic thermosets provide an exceptional medium for thermal and ablative protection, particularly when formulated into composite parts utilizing carbon and silica cloth reinforcements. For the carbon cloth phenolic (CCP) composites used in RSRM exit cone panels, the mechanism of phenolic carbonization becomes an extremely important process to understand and monitor.

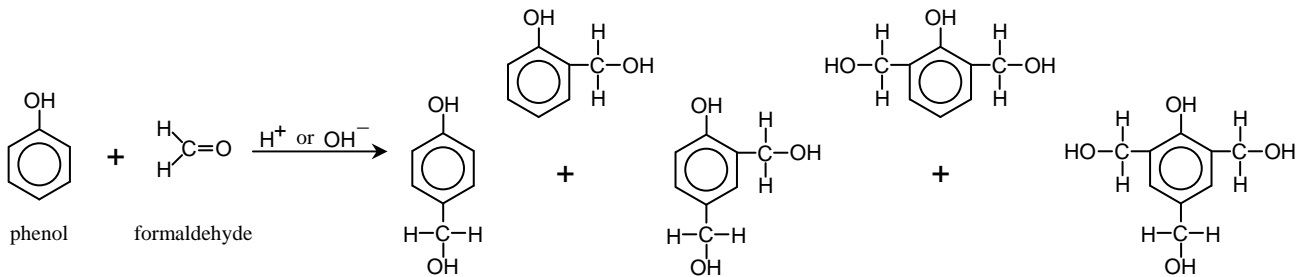
Over the years, a number of studies have been published examining the thermal performance characteristics of phenolic resins and phenolic-based composites using a variety of analytical tools. In particular, Thermogravimetric Analysis (TGA) systems as well as TGA instruments coupled with other analytical devices such as Mass Spectrometers (MS) and Gas Chromatographs (GC). While stand-alone TGA instruments monitor weight changes that occur as samples are thermally degraded over specified heating rates, TGA-MS and TGA-GC coupled systems permit qualitative and quantitative analysis of the gaseous components released during the decomposition process. These types of instrumental approaches are enormously beneficial in helping to understand the decomposition mechanisms and reaction kinetics involved in the thermal conversion/degradation process.

In this first report examining basic phenol-formaldehyde resin chemistry and subsequent decomposition mechanics, the intent is to deal only with the phenolic matrix component of these composites in terms of its decomposition chemistry under ordinary heating conditions, in essence, to lay the ground work for future studies by examining some of the more traditional elements of phenolic degradation. Future efforts may consider other components in the system or the composite itself and will focus on the properties and behavior of these materials under more extreme conditions of heat and pressure, analogous to the carbon fabric / phenolic matrix ablative structures used in flame-exposed exit nozzle assemblies. No specific tests were performed nor was any experimental data specifically acquired for this study. Rather, this first paper makes use of information already available from previously published sources as well as previous studies conducted by the author which involved the processing, characterization and formulation of phenolic thermosets under in similar conditions.

While many of the points emphasized here are common knowledge or can be verified, some of the analysis and characterizations are speculative and may include perceptions or suggestions based strictly on the author's perspective and background. No guarantee is made as to the correctness of any of these suggestions. They are offered merely to provide possible explanations for some of the questions that arise when evaluating the complex mechanisms associated with phenolic decomposition processes. For this current study, use of specific data and experimental results from other publications as well as previous research activities are utilized and so noted. Additionally, all reaction pathways, reaction mechanisms, derived equations and associated kinetics presented in this paper are strictly the author's perception and opinion. Eventually, it is hoped that some of these techniques can be expanded, further developed and effectively adapted to provide some meaningful insight into nonmetallic nozzle components for future high temperature applications.

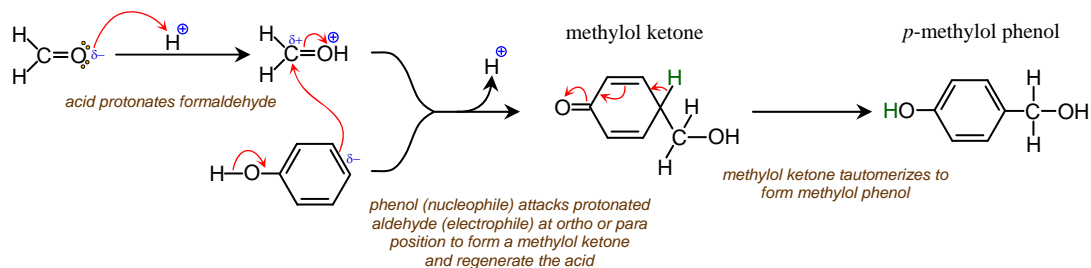
## Phenol-Formaldehyde Resin Chemistry

In order to enhance understanding of cured phenolic bodies undergoing thermal decomposition or conversion into char, it may be beneficial to review some of the text book chemistry behind the synthesis of these resins. In general, the primary monomeric reactants, phenol and formaldehyde, are first reacted to a small degree to produce a mixture of 'pre-polymers' (oligomers). Several functional variations are available during the production of phenol-formaldehyde (phenolic) resins depending on their specific end-use applications. For products requiring high carbonaceous resins, such as those bound for aerospace and high temperature applications, the common route is the production of *resol* precursors (or oligomers) via reaction between phenol and formaldehyde under acidic (or basic) conditions to form hydroxymethylphenols (or methylol phenols) . . .

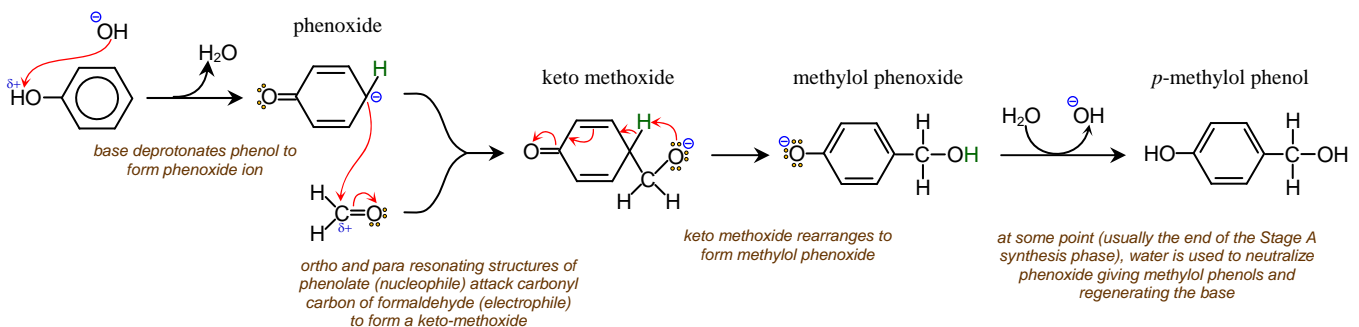


mixture of ortho and para mono, di and tri methylol phenols

The phenol hydroxy group directs substitution at the *ortho* and *para* ring positions and the specific methylol products prepared depend on the formaldehyde-phenol ratio which can range from about 1:1 to 1:3<sup>[1]</sup>. These compounds can be generated in acid or basic media via electrophilic aromatic substitution. Catalyzation by acid leads to novolac resins while base catalysis forms resols. In either case, the reaction scheme indicates the release of water, thus both mechanisms are considered to be *condensation*. During the production of novolacs, formaldehyde is protonated to form an electrophile which is attacked by the nucleophilic phenol ring generating a methylol ketone which finally tautomerizes to produce ortho and para methylol phenols . . .

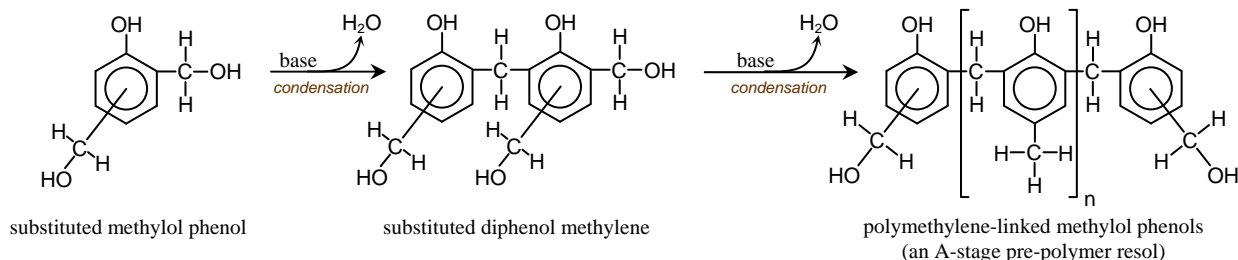


. . . while in alkaline media, base (OH<sup>-</sup>) deprotonates phenol to form phenoxide which attacks formaldehyde to give methylol phenoxides. Ultimately, these yield methylol phenols when washed (neutralized) with water . . .



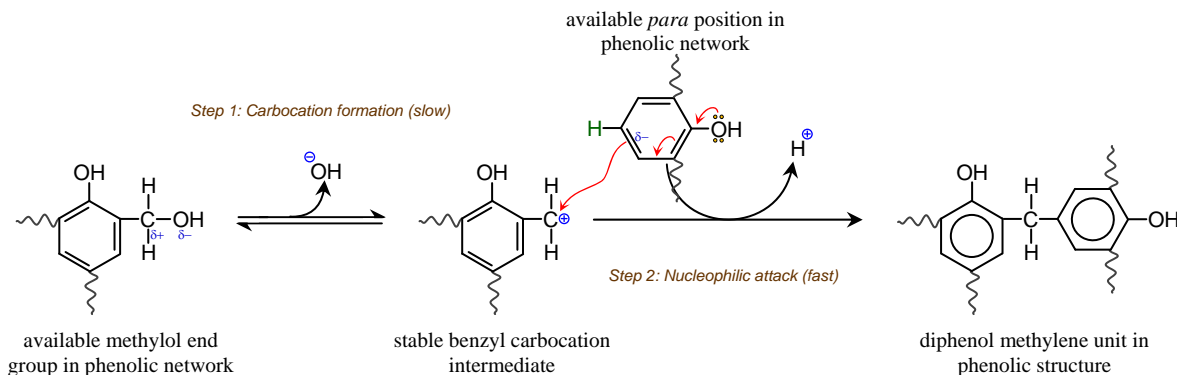
Methylol phenol precursors can then react with phenol, formaldehyde or with themselves via water-producing condensation reactions. Of primary interest here are the resol mixtures which initially form dimers and trimers of methylene-linked and methoxy-linked phenols such as dihydroxy mono and di substituted phenyl methanes and ethers (substituted diphenol methylenes and ethers) which undergo step-growth polymerization into substituted poly phenol methylene-linked oligomers (A-staged pre-polymers) . . .

#### Production of Stage A Phenolic Resol

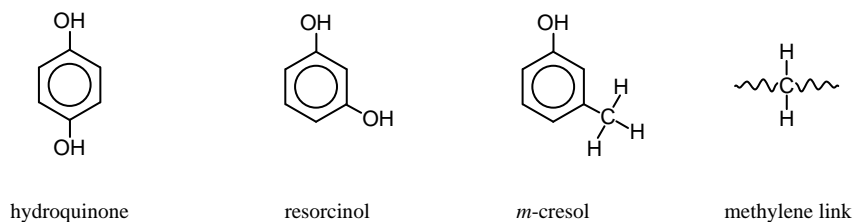


In this scenario, it is surmised that available methylol groups on branch and end segments within the phenolic adduct dissociate into electrophilic carbocation sites which then undergo  $S_N1$ -type substitution with local or neighboring phenol rings containing unreacted nucleophilic *ortho* and *para* positions. Here, diphenol methylene units are formed as the phenolic polymer develops with the release of water at each reaction site . . .

#### Mechanism for $S_N1$ Phenolic Polymer Development



Number average molecular weights of Stage A phenolic resol resins might range from about 100-500 with viscosities perhaps in the 30-300cps range. Stage B resins are the primary industry forms of these resins as the degree of polymerization is advanced and viscosities reach into the thousands. B-staging treatments and processes may be initiated by the resin manufacturer but are usually carried out by the end users and broadgoods processors. For instance, prepreg vendors may B-stage their materials after impregnation with A-stage resin and shop fabricators may perform B-stage processing on composite lamina and other phenolic build-ups during their manufacturing processes to enhance handling, curing, resin distribution and cured physical properties. Custom phenolic resin formulations may include other monomers which enhance reactivity and perhaps lower curing energy requirements. Some of these constituents might include resorcinol, hydroquinone and/or cresol (all three of which are more reactive than straight phenol, particularly resorcinol and *m*-cresol). Some of these reactants have been detected in previous studies <sup>[2]</sup>.



The overall resin processing sequence can be represented by the following diagram . . .

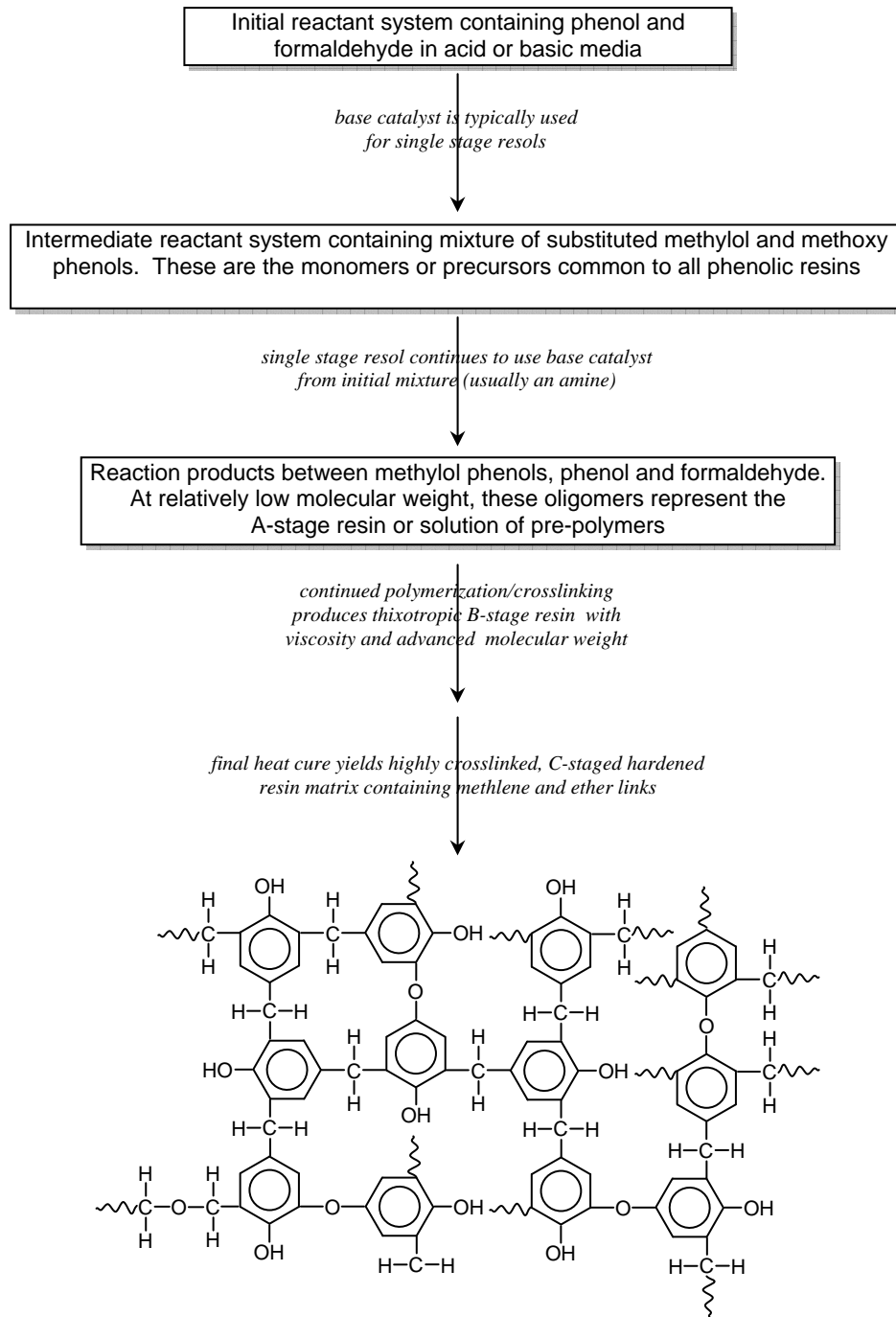


Figure 1. Suggested representation of an idealized cured phenolic resin structure.

For fully cured systems, the idealized structure given in Figure 1 will be dominated by methylene links joining phenol rings along with lower levels of (1) methoxy-type ether links formed during the initial reactions which are still present due to shielding from subsequent heating conditions, and (2) phenoxy-type ether links occasionally formed between neighboring phenol hydroxy groups. In both cases, these ether groups are vulnerable to dehydration, oxidation, dehydration or advanced condensation reactions. Subsequent post-curing to 450°500°F will remove essentially all the ether links as formaldehyde is generated.

## Carbonization Mechanisms & Degradation Pathways

### *Structure of Highly Crosslinked Carbonized Thermosets*

Graphite is one of the most well known forms (allotropes) of carbon. The anisotropic, hexagonal close packed structure with characteristic '*d*' spacings are responsible for many of its unique properties. These '*d*' links, connecting planes of hexagonally bonded carbon atoms by way of van der Waals forces, permit slipping between the planes (hence, graphite's lubricating properties) and ultimately affect the thermal conductivity and thermal expansion characteristics quite differently than the other forms of carbon. Carbon atoms in these planes are covalently bonded to three other carbons via trigonal  $sp^2$  hybrid orbitals and donate a fourth  $\pi$  electron to the delocalization pool responsible for graphite's high conductivity along these planes.

On the other hand, amorphous carbon structures being joined via tetrahedral  $sp^3$  orbitals may include forms of carbon black, petroleum coke, 'green' cokes and the carbonized form of coal tar pitches. These more common amorphous allotropes are considered to be 'soft' carbons, a term that is used by carbon scientists for carbon structures that crystallize/graphitize when heated to temperatures  $> 4000^\circ\text{F}$  (at ambient pressures). During early heating cycles, soft carbons will go through a temporary mesophase (or liquid crystal) state somewhere in the range  $750\text{-}950^\circ\text{F}$ . Mesophase networks exhibit a certain degree of mobility which facilitates the formation of graphitic layer planes or graphene layers eventually leading to a pre-graphite lattice. Continued heating into graphitization temperature ranges ( $4000^\circ\text{-}4500^\circ$ ) converts amorphous  $sp^3$  bonded regions into  $sp^2$  configurations and the network begins to become rich in aromatic  $sp^2$  orbitals. Unless oxidation pre-treatments are applied (a process called oxidative stabilization), all graphitizable carbon forms must pass through this mesophase state before developing substantial hexagonal  $sp^2$  character.

Now the char remnants of densely crosslinked thermoset polymers comprise a unique category of amorphous carbon, often referred to as 'hard' carbon. In contrast to soft carbons, the term 'hard' typically means that no movement or rearrangement of the atoms occurs during heating. Consequently, hard carbons will not undergo reconstructive transformation under ordinary graphitization conditions. The atoms in the organic precursor to these types of non-graphitizing structures are permanently fixed in space due to the heavily crosslinked and interconnecting network established during the curing process. Most thermoset plastics, particularly cured phenolic resins, form very hard carbons upon carbonization. These carbonaceous materials are also termed 'glassy' or 'vitreous' carbon since they appear to contain very high degrees of amorphism and exhibit fractured faces characteristic of glass materials. Some of the properties of glassy carbons include: thermal resistance up to  $\sim 6000^\circ\text{F}$  in inert atmospheres, mechanically hard and brittle (like a ceramic), low thermal conductivity (compared to all the other carbon forms), high resistance to thermal shock (compared to all the other carbon forms), and often has the appearance of a 'black glass'.

Many thermoplastics, most linear aliphatic polymers, as well as simple and fused aromatics will readily undergo graphitization while most thermosets (such as phenolic resin) will not graphitize even at temperatures of  $5500^\circ\text{F}$  and above. In addition, contrary to industry perceptions as well as many information sources, cyclic aliphatic structures, such as rayon and PAN carbon fiber precursors, contain only limited amounts of semi-graphitizable segments. While these forms may include substantial amounts of 2-D graphene planes, they are more properly classified as hard, non-graphitizable carbons. In general, transformation of solid precursors produces hard carbons. The difference between graphitizable and non-graphitizable carbon can be appreciated visually by examining Figure 2 below, courtesy of some of the research done by Peter Harris<sup>[3]</sup>, which shows images of (a) sucrose and (b) anthracene carbonized at  $4200^\circ\text{F}$ . Note that anthracene is analogous to coal tar pitch, which easily graphitizes, and sucrose (a polysaccharide sugar made up of glucose and fructose) which is similar to non-graphitizable rayon (a polysaccharide formed from beta-bonded (cellulosic) glucose units).

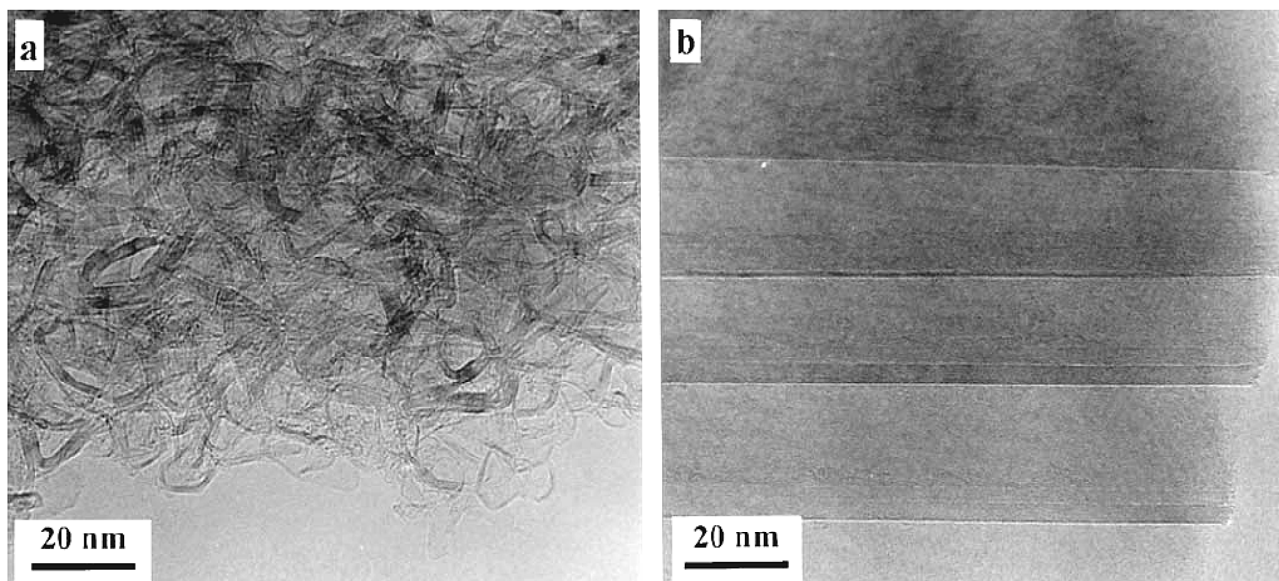


Figure 2. Micrographs of (a) sucrose carbon and (b) anthracene carbon following heat treatment at 4200°F.

Carbonized phenolic resins visibly retain a substantial resemblance to the amorphous isotropic character formed during cure of the organic phase. Glassy chars formed from thermoset polymers may include porosity developed during the pyrolysis process and/or widening and extension of the interconnecting pore structure created during the condensation curing process. Pore structure in glassy carbons appears to be highly influenced by the specific conditions implemented during the cure process (such as applied pressure and heating rate during autoclave cure). Independent observations over several years have indicated that the pore macro-structure is essentially established during the polymer curing stage (or article fabrication process), and the escape of pyrolysis gases appears to occur predominantly as these existing pores are widened and enlarged. In addition, abrasive diffusion or etching as pyrolysis gases strive to exit the system can create micro-porosity which interconnects to and essentially becomes an extension to the existing pore network. Gases that are unable to diffuse, escape, or etch their way into existing pore channels may form regions of 'closed porosity', and the fraction of closed porosity (out of the total porosity) is difficult to surmise, as is the permeability fraction. Inevitably, contraction stresses develop that can sometimes cause fracturing of the brittle phenolic char during the cool down phase.

Thermoplastics and soft carbons are often subjected to low temperature oxidation treatments to convert their structures into non-flowing graphite precursors which bypasses melting and mesophase formation. Most of the common thermoset polymers, such as epoxies and urethanes, contain too much oxygen and/or nitrogen along the polymer chains to make acceptable char precursors, and they tend to produce highly fragmented char remnants with extremely low char yields. In terms of carbon yield, thermal resistance, oxidation and ablative protection, resins made from phenol-aldehyde and furfuryl alcohol are the best carbonizing polymers available. It should be realized that the carbonization process transforms an organic material into an inorganic carbon form, and likewise, the methods for describing these two phases must transcend from organic to inorganic chemistry . . . almost.

## *Oxidation and Pyrolysis are Parallel Processes*

One must realize that the structure of phenolic substrates contains reaction water, absorbed moisture, hydroxyl groups, perhaps air pockets and other sources of oxygen. Thus, to varying degrees, oxidation/combustion and inert pyrolysis must be coexistent processes during the thermal decomposition process, especially in the early degradation stages. Even during a pyrolytic operation conducted entirely under inert conditions, initial decomposition reactions will inevitably include oxidation of the phenolic matrix. Universally, the combustion products of organic matter are typically water and carbon dioxide. Also, as inert pyrolytic decomposition progresses, oxygen radicals are generated which will induce oxidation reactions with polymer sites on their way out. In an oxidizing environment on the other hand, combustion is obviously a major player in the decomposition process, but pyrolysis is also taking place in regions of the network where oxygen is not present or has been 'starved' out of the network, and this can be substantial.

No doubt, the higher the degree of pyrolysis, the greater the char yield will be. In a number of previous studies conducted by the author examining Borden resols<sup>[2]</sup>, neat phenolic resin samples cured under pressure have repeatedly yielded around 56% char remnant after almost complete conversion (95-98%) and a measured true density of 1.43g/cm<sup>3</sup>. Literature TGA results have frequently noted ~ 50% char yields for cured phenolic resins<sup>[4]</sup>. Without the application of pressure during the curing cycle, the release of solvents and condensation volatiles can become somewhat violent after about 200°F resulting in significant resin loss. Decomposition products for oxidation and pyrolysis have some significant differences in the types of gaseous molecules emitted during the process. It goes without saying, decomposition gases are the sole reason for weight losses that occur during TGA tests and carbonization applications, regardless of the amount of solid char produced. While composition differences in char yield may be small for the two degradation processes, inert pyrolysis will favor the generation of carbon monoxide along with various hydrocarbons reflective of the original phenolic structure while oxidation and combustion will be characterized primarily by the release of CO<sub>2</sub> and water.

Thus, a proper treatment of the thermal degradation of phenolic networks must take into account the reactions and effects of both pyrolytic and oxidative degradation concurrently as well as independently, regardless of the decomposition environment and specific firing conditions. The majority of TGA-MS evidence indicates (at least to this author) that oxidation is predominant during the first portion of the decomposition process and then pyrolysis products (cracking) tend to dominate the higher temperature portion of the cycle. Oxidation and pyrolysis reactions may appear to be consecutive phases from one perspective but they definitely have significant overlaps across the decomposition process. This point will be explored further later on.

## *Thermal Decomposition Kinetics of Phenolic Polymers*

It has been demonstrated that the thermal decomposition kinetics of cured phenolic networks are greatly influenced by the heating rate used during the carbonization process, particularly between about 300°C/min (570°F/min) and 500°C/min (930°F/min)<sup>[5]</sup>. A number of TGA techniques are available to explore a variety of interesting test conditions during the heating cycle that can reveal much information about the mechanisms at work during the thermal decomposition process. Phenolic matrix composites used in ablative and nozzle liner applications see abnormally high heating rates (several thousand degrees in a couple of minutes) and it is not unusual for classical kinetics and thermochemistry expectations to fall short of a reasonable description of the actual phenomena taking place. Rapid carbonization and thermal shock effects are the primary topics for future studies in this series. This first paper is intended to explore

the more classical approaches in describing the behavior of phenolic networks during carbonization and may serve as a starting point or baseline, if you will, for developing more appropriate models to better define the extremely rapid conversion of these materials during the rocket firing process.

One thing is fairly certain however . . . regardless of whether the firing sequence is fast or slow, *the thermal degradation of phenolic polymers is a temperature driven, free radical propagating process.* During the initial decomposition phase for a slow, steady state firing cycle, stable radicals will naturally form, rearrange and seek low energy states in accordance with classical thermodynamics. However, as the system temperature relentlessly increases throughout the heating cycle, less stable radicals become the inevitable intermediates and decomposition pre-products begin to deviate substantiately from traditional organic reaction analogs. Indeed, the lifetimes of transition state free radicals during solid state thermal conversion of plastic thermosets must be abnormally high.

Free radical chemistry is an extensive subject (and quite popular in recent years) dealing heavily with the concept of a single or lone electron in a given atom or molecule, and often treats di- and tri-radical species in special situations. In contrast, decomposition of a cured phenolic article (one big solid molecule) might contain thousands of reaction sites where free radicals are being generated as the network begins to break down into smaller contiguous fragments. Any given fragment would contain a multitude of cleavage points in which radicalized molecular groups are undergoing simultaneous decomposition reactions. In addition, it is suggested here that, during later stages of the decomposition process, single carbon atoms may themselves assume short lived tri- and quad-radical transition configurations. These concepts give new meaning to the term ‘di-radical’.

From a simplified perspective, thermal decomposition of a phenolic network might be represented as a two step, first order, unimolecular, irreversible reaction. As decomposition commences, the cured polymer  $P$ , degrades to form free radical intermediates  $I\cdot$ , which then react to produce carbonized resin char  $C$  and pyrolysis/combustion gases  $G$ . To be thorough, at least two cases should be considered: (a) the radicalized intermediates are converted into char along a reaction path that also generates gases, and (b) the intermediate is converted into gases and char along independent pathways in parallel reactions. Another scheme might combine both cases as coexistent and/or parallel processes. This is probably more reflective of reality but is beyond the scope of this first report. For the present, consider the situation given in (a) . . .



In this scenario, the quantity of phenolic substrate decreases as free radical intermediates are generated and the concentration of radical intermediates decreases with the simultaneous formation of gases and solid resin char. Kinetically, the rate equations can be given as . . .

$$\frac{dP}{dt} = -k_p P \qquad \frac{dI\cdot}{dt} = k_p P - k_{CG} I\cdot \qquad \frac{dC}{dt} = \frac{dG}{dt} = k_{CG} I\cdot = k_{CG} CG$$

In some problems, the steady state approximation can be applied. The theory presumes that the change in intermediate free radical concentration remains constant so that  $dI\cdot/dt \approx 0$ . This condition gives simply,  $k_p P = k_{CG} I\cdot$  and  $dC/dt = dG/dt = k_p P$ . Now if  $W_0$  is the initial weight of a TGA sample and  $W$  is the instantaneous weight as the sample undergoes conversion, then  $W_0 = P_0$ ,  $W = P + C$  and  $W_0 - W = G$ . Here, the degree of conversion shall be defined as  $\alpha = 1 - W/W_0$  or  $\alpha = 1 - W$  if the weight is normalized. Then the rate equation can be given as . . .

$$(1) \quad \frac{d\alpha}{dt} = k(1-\alpha)^n$$

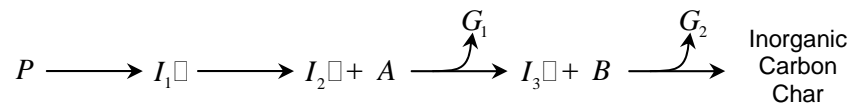
which becomes

$$-\frac{dW}{dt} = kW^n \quad (2)$$

where  $n$  represents the order of the reaction.

The assumption of steady state conditions is prevalent throughout the literature for many situations involving burning/combustion processes, pyrolysis and TGA of polymers. However this simplification may be invalid for applications dealing with abnormally high heating rates and rapid firing situations. These conditions will be dealt with in future studies.

Before proceeding, it should be noted that the reaction scheme given above is probably over simplistic. It is more likely that the actual mechanism involves the concurrent production of multiple gases, several intermediate radicals and a few compounds along any given pathway leading from the organic polymer state to the final char. Perhaps something like . . .



Now when the heating rate is known or specified,  $\beta = dT/dt$ , and the well known Arrhenius temperature dependency is incorporated into Eq (2), the result becomes . . .

$$\frac{-dW}{dT} = \frac{A}{\beta} \exp\left(\frac{-E_a}{RT}\right) \cdot W^n \quad (3)$$

where, as usual,  $A$  is the pre-exponential factor,  $E_a$  is the activation energy for the reaction (or group of reactions),  $R$  is the gas constant ( $8.3144 \text{ J}^\circ\text{K}^{-1}\text{mol}^{-1}$ ) and  $T$  is the absolute temperature. This relation can be applied to dynamic TGA curves as will be attempted below. One must realize however, Eq (3) reflects the weight losses occurring due to generated pyrolysis gases and says nothing (that is, directly) about the char solids that are produced.

The kinetics of free radical polymer decomposition is a tricky subject due to the large number of possible conditions and parameters, each of which can have significant effects on the apparent reaction rates and activation energies. Even the particular kinetic model or analytical approach used can give vastly different results than another model. Thermal decomposition of phenolic networks via TGA has been the subject of many studies over the years with the majority of those cases examining conditions of relatively slow, steady state conversion of small resin samples. In previous studies examining one of the Borden resol resins (the predecessor to Durite SC1008HC) a number of chemical/physical characterization methods were utilized including a series of dynamic TGA measurements conducted in nitrogen atmosphere<sup>[2]</sup>. Some of those results have been reproduced here and are presented in Figures 3 and 4 which clearly illustrate the primary weight changes taking place when neat phenolic resin samples are heated from room temperature up to about 1500°F at 20°/min (~0.3°/sec). In these tests, the resin sequentially underwent (1) complete solvent evaporation, (2) full condensation cure and (3) pyrolytic decomposition in about a 40 minute time span.

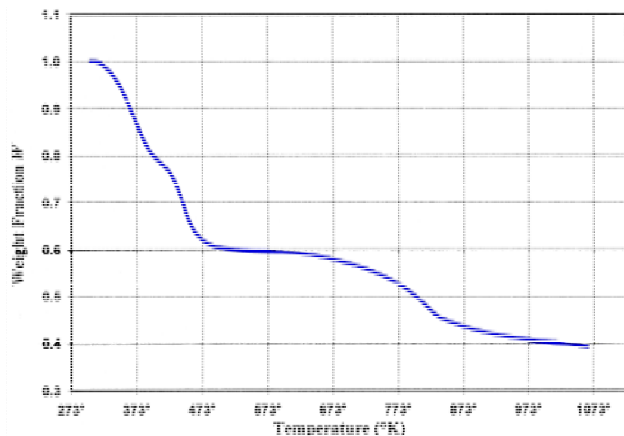


Figure 3. Dynamic TGA trace showing weight change vs. temperature for Borden phenolic resin.

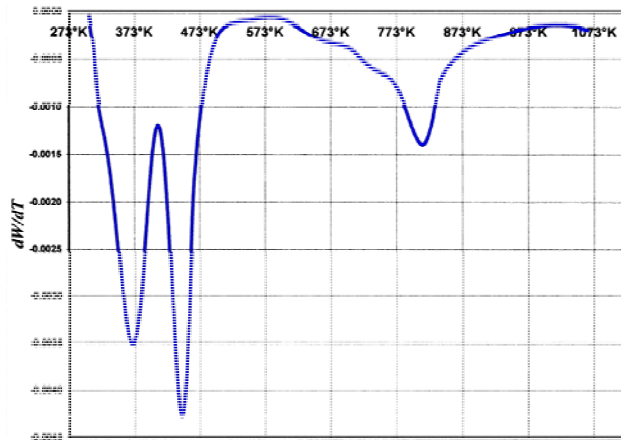


Figure 4. Derivative curve (dTGA) for TGA trace given in Figure 1 highlighting regions of maximum weight loss.

The first derivative curve shown in Figure 4 (denoted dTGA or  $dW/dT$ ) illustrates the regions of primary weight loss across the applied temperature range where the peaks represent the inflection points along the original TGA curve. Moving from left to right (Figure 4); the first peak depicts the release of resin solvent (IPA) commonly used in HS resins at about a 30% level (boiling point 355°K); the second peak illustrates the condensation (polymerization/crosslinking) reactions that result as the resin undergoes thermal curing; and the last, broader peak, starting at about 580°K, represents the thermal decomposition range which includes pyrolytic conversion of the cured resin into glassy carbonized char and pyrolysis volatiles. More precisely, peak one is a measure of the weight loss that occurs as IPA boils out of the system, peak two measures the weight loss from the release of condensation side product (water), and the third region depicts weight losses occurring as gaseous pyrolysis side products leave the system. Since the thermal decomposition (pyrolysis) process is the region of interest, it is worth while to study this region in greater detail. Figure 5 is a blow up of this range which highlights some special points of interest.

Examination of Figure 5 below permits the following observations. Prior to the primary region where the majority of decomposition occurs (midpoint 812°), there appears to be two minor sub-regions where perhaps early decomposition reactions are taking place, suggesting that the degradation process consists of at least three phases. Moving from left to right, let us denote these sub-regions as A, B and C respectively. The peaks or midpoint temperatures are indicated for each sub-region and reflect the point of maximum weight loss occurring in those sub-regions across the TGA test range. Notably, sub-regions A and B are not so apparent in the original TGA trace but are visibly detectable in the dTGA curve. As will be expanded on later, sub-region A (and maybe some of B) is believed to represent secondary combustion/oxidation reactions that precede or lead into the primary pyrolytic decomposition phase C. However, one should bear in mind the that there is a considerable degree of overlap between the combustion and pyrolysis phases.

Many authors throughout the literature have utilized various forms and modified versions of Eq (3) by surmising reactions orders that were fractional and/or negative. Incremental activation energies

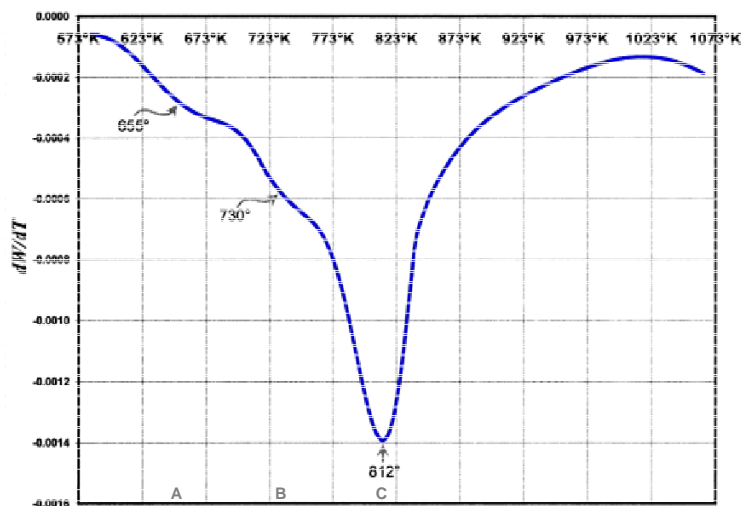


Figure 5. Decomposition region of dTGA curve given in Figure 2 showing particular points of interest.

can indeed exhibit non-integer and negative values in complex multi-step reaction sequences. However it is contended for this simplified first attempt, that all the reactions (and steps) of interest during this analysis follow first order kinetics in which the value of ‘1’ is used throughout. Should this approach become insufficient, more complex orders can be considered at a later time. The universal validity of Eq (3) across a broad spectrum of temperatures and reaction types could be debated with good reason however, its application to particular elements in this study have appeared to provide some useful information. Each sequence of reaction steps in a given phase will have a unique value for  $E_a$  and  $A$  where the sum of the three phases should give the overall  $E_a$  for the entire decomposition process (across the temperature range examined).

Now consider our basic rate equation, Eq (3) with  $\beta = 0.3^\circ\text{K}/\text{sec}$  and  $n = 1$ . As is commonly done, the equation is written in linear ‘slope-intercept’ form by taking logs . . .

$$\ln\left(\frac{-dW/dT}{W}\right) = -\frac{E_a}{R} \frac{1}{T} + \ln\left(\frac{A}{0.3}\right) \quad (4)$$

If applied intricately, this linear form of the weight-temperature rate law can be plotted and used to infer approximations for  $E_a$  (a component of the slope) and  $A$  (a component of the y-intercept) along segments where approximate ‘Arrhenius linearity’ prevails. Close examination of Figure 3 seems to indicate that the most linear segments in dTGA occur prior to the TGA inflection points, midway between the start of each region and the maximum temperature points indicated. These particular segments represent the areas of maximum ‘acceleration’, if you will, for each region since they are the steepest down ramps occurring prior to the point of maximum weight loss. These acceleration points can be guessed from the dTGA curve or better yet, determined more precisely from the second derivative curve (denoted  $d^2\text{TGA}$  or  $d^2W/dt^2$ ) given in Figure 6 below which illustrates the inflection points of the dTGA curve for sub-regions A, B and C.

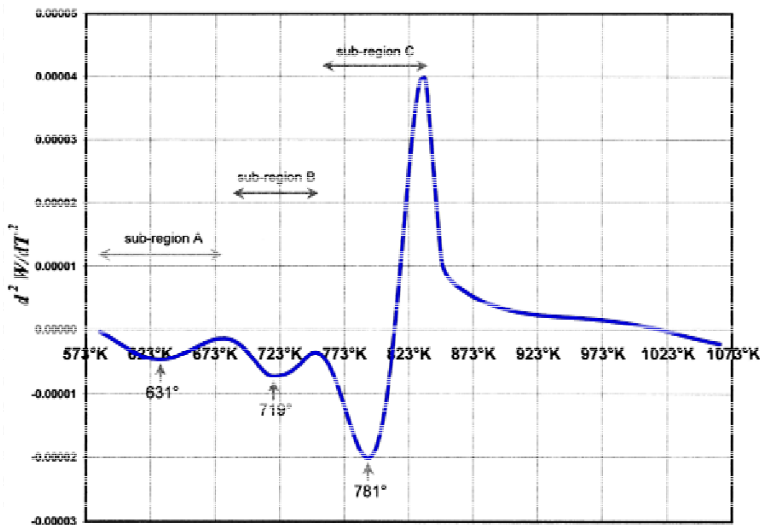


Figure 6. Second temperature derivative curve for the initial TGA trace indicating dTGA inflection points in the maximum acceleration segments of each sub-region.

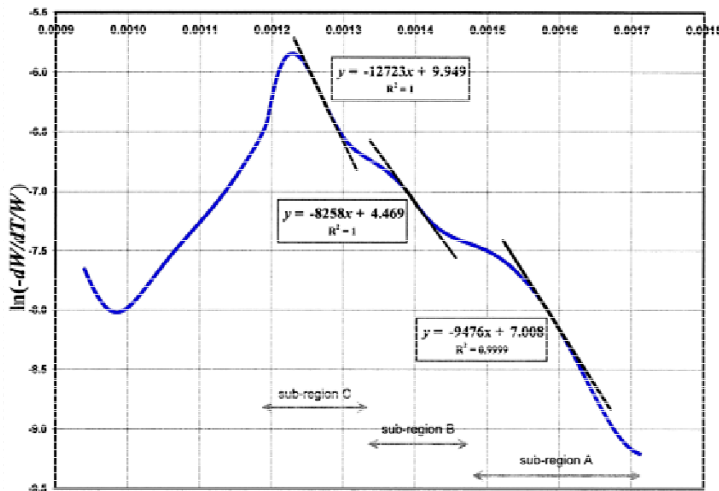


Figure 7. Composite plot of Eq (3) vs.  $1/T$  across the entire decomposition range showing analysis of tangent lines at maximum acceleration points for each sub-region.

Table 1. Results from linear tangent analysis of TGA data for Borden resol over three sub-regions within the decomposition process.

	A	$E_a$
	A	$E_a$
Sub-Region A	$3.68 \times 10^2 \text{ sec}^{-1}$	$78.8 \text{ kJ mol}^{-1}$
Sub-Region B	$2.91 \times 10^1 \text{ sec}^{-1}$	$68.7 \text{ kJ mol}^{-1}$
Sub-Region C	$6.98 \times 10^3 \text{ sec}^{-1}$	$105.8 \text{ kJ mol}^{-1}$

Overall  $253.3 \text{ kJ mol}^{-1}$

In a composite plot containing all three sub-regions, linear tangent lines at each of the dTGA maximum acceleration points (as highlighted in the  $d^2TGA$  curve of Figure 6) can then be simultaneously evaluated to the linear form of Eq (4). A graph of . . .

$$\ln\left(\frac{-dW/dT}{W}\right) \text{ vs. } \frac{1}{T}$$

across the entire decomposition range is given in Figure 7 along with the tangent line analysis used for each sub-region as determined via linear regression techniques. With this method, the slope of the tangent line for each sub-region is equal to  $E_a / R$  and the y-intercept is simply  $\ln(A/0.3)$ . Results from the analysis are given in Table 1 where independent values for each of the sub-regions are estimated along with the overall activation energy for the process (the total  $E_a$ ).

While the method applied here is not commonly pursued during traditional kinetic studies, it is felt this approach, as illustrated in Figures 4 and 5 and Table 1, provided good results for  $E_a$  at the expense of accuracy in the value for  $A$ .

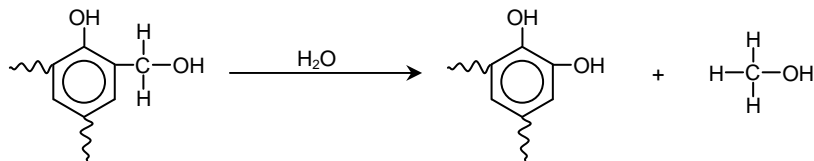
These parameters have been determined by a number of authors over the years. A couple of those can be noted here. Using TGA methods at various heating rates up to  $160^\circ\text{C}/\text{min}$ , Moore, Tant and Henderson<sup>[6]</sup> determined an overall activation energy of  $269 \text{ kJ/mol}$  on phenolic ablative materials. Also, applying a rate of  $1^\circ\text{C}/\text{min}$  in air and using three different kinetic models, Ninan<sup>[7]</sup> estimated values of  $77.7$ ,  $81.2$  and  $102.8 \text{ kJ/mol}$  for the  $E_a$  of glass/phenolic ablatives.

In a study by Chang and Tackett<sup>[4]</sup>, samples of cured phenolic resin were subjected to TGA-MS in efforts to characterize the material throughout the decomposition process. One of the most interesting results from this study was the analysis of pyrolysis gases released while the polymer was heated to about 1400°F at a rate of 40°/min in He resulting in a 50% char yield. For this current paper, we have taken some of their results (TGA weight loss data and MS trace ion curves) and formulated a new table to contain, not only the compound weights detected and corresponding peak temperatures, but also the estimated molecular fractions and temperatures pertaining to the apparent start of weight loss for each compound detected. These results with a few notes are given in Table 2 below.

Table 2. TGA-MS results for cured phenolic resin samples showing pyrolysis/oxidation gases released during TGA heating to 1400°F at 40°F/min in He . Data extracted and modified from study by Chang and Tackett.

	50% of TGA Weight Loss %	Estimated Mole Fraction %	Peak Temperature °F	Start Temperature °F	Comments and Notes
water	0.8	2.49	248°	-----	peaks & start points coincide
phenol	0.3	0.18	293°	-----	
water	4.4	13.7	410°	338°	
phenol	1.8	1.07	410°	338°	
methanol	1.2	2.10	410°	338°	
carbon dioxide	0.4	0.51	410°	338°	
ammonia	2.7	8.91	518°	410°	peaks & start points coincide
unidentified	0.3	0.42	734°	653°	
water	5.0	15.6	824°	698°	peaks & start points coincide
carbon dioxide	0.7	0.89	824°	698°	
water	5.7	17.8	1148°	995°	peaks & start points coincide
carbon dioxide	1.3	1.66	1148°	995°	
methane	3.8	13.3	1238°	986°	peaks only coincide
benzene	3.4	2.44	1238°	824°	
toluene	2.7	1.61	1220°	932°	methane emitted to 1400°
xylene	1.3	0.69	1211°	986°	
trimethyl benzene	0.2	0.09	1202°	-----	
phenol	4.1	2.45	1292°	806°	peaks & start points coincide
cresol (methyl phenol)	2.6	1.35	1292°	806°	
dimethyl phenol	1.1	0.51	1328°	-----	rapid drop after peak
trimethyl phenol	0.1	0.04	1328°	-----	
carbon monoxide	6.1	12.2	1382°	990°	
	50.0	100.0			

Consider the components detected up to about 650°-700°F. First, it is believed that the production of water up to this temperature range is primarily a result of continued curing and advanced condensation reactions within the phenolic network leading to further crosslinking and the release of residual volatiles. However, water is also produced during the early degradation phase when oxidation/combustion reactions are taking place. Smaller molecules, such as phenol and methanol are hydrogen bound until the thermal energy allows their expulsion. Free phenol is released from the resin and immediately volatilizes along with trapped moisture, CO<sub>2</sub> and methanol. The presence of methanol in the resin solution could be due to earlier reactions involving hydrolysis of unreacted methoxy groups within the polymer adduct . . .



or simply by hydrolysis of free formaldehyde with the production of  $\text{CO}_2$  . . .



Amine-based compounds are common catalysts in phenolic resin systems. At high enough temperatures, unreacted portions of these catalysts will begin to break down releasing ammonia. Other resin components might include trace amounts of activators (metal chelates for instance), oxidation inhibitors or perhaps wetting agents. Beyond about 700°F, degradation of the organic network commences and the polymer phase begins to lose its identity.

It should be noted that MS will not detect anything below about 10 MW units, thus hydrogen, which we know is generated during the carbonization process, is not indicated at all in these results. Studies by other workers utilizing chromatography techniques have demonstrated elemental hydrogen to be a major pyrolysis constituent. For instance, using other techniques in addition to MS, such as Gas Chromatography (GC), Thoeni, Baker and Smith<sup>[8]</sup> reported a hydrogen emission level of approximately 25% of the total TGA weight loss for samples of urethane-furfuryl polymer, in addition to the expected pyrolysis/oxidation products emitted, ie...  $\text{CO}_2$ , CO, methane and monomeric derivatives of the polymer tested. Table 3 is a duplication of their results and reveals that a portion of the hydrogen was released in the 700°-1200°F range while most was detected at higher temperatures.

Table 3. TGA-GC results for urethane-furfuryl alcohol samples evaluated by Thoeni, Baker and Smith indicating decomposition gases evolve. Of particular interest here is the hydrogen generated during the process.

	Quantity Volatilized (in cm <sup>3</sup> /g of initial sample)			
	80 - 400°F	400 - 730°F	730 - 1255°F	1255 - 1920°F
carbon dioxide	4.5	27	10	2.1
carbon monoxide	0.016	1.8	20	8
hydrogen	-----	-----	28	75
methane	-----	0.42	28	4.5
hydrogen cyanide	0.01	0.01	0.13	1.3
furan	0.05	0.04	0.2	0.02
tetrahydrofuran	0.2	0.4	0.9	1.8
light hydrocarbons	0.12	0.3	4.2	3.7

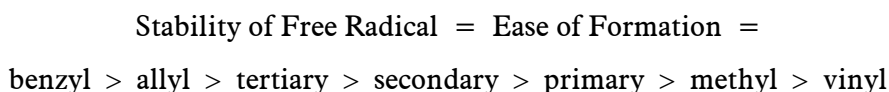
To avoid confusion with our current study, note that the appearance of cyanide and furan in Table 3 are reflective of the particular polymer these researchers investigated – Table 3 provides its benefit by demonstrating that, with little doubt, hydrogen is a major player in the decomposition process, especially at higher temperatures. A thorough analysis of the decomposition gases would require both MS and GC.

Without information such as that reported in these two studies, a meaningful understanding of the decomposition process is rather vague. Our objective now is to identify and formulate likely carbonization mechanisms and reaction pathways by accounting for some of the major components listed in Table 2 during the decomposition phase (that is, after about 700°F) in conjunction with the production of hydrogen and solid char. This analysis will be developed over the next few sections.

## *Sequence of Bond Cleavage and Free Radical Generation*

Thermal degradation of polymers starts with bond-breaking reactions (homolysis) to form free radicals as primary products. In the phenolic macromolecule, there are many different types of bonds and related bond dissociation energies. One might ask, which bonds go first or which bonds represent the weakest links? And just as importantly, at what point does the network transform from an organic polymer into an inorganic char? Undoubtedly, in the distribution of heat throughout the polymer network, some of the stronger bonds will absorb enough energy to rupture while in other areas, some of the weaker bonds remain intact. Also, it must be realized that in a system continuously increasing in temperature (such as a heating cycle, for instance), the sequence of bond breaking is substantially augmented according to the specific time-temperature profile employed.

For a system comprised of a several types of bonds, a good indicator of relative bond strengths can be inferred by the energies of the specific free radicals generated during the homolysis step. Generally, each cleavage within the structure will produce two radicals, and the more stable the radicals, the more likely the reaction. Basic energetics teaches that the ease of formation of free radicals follows directly with their stability. Recall for instance, benzyl radicals are more stable than alkyl radicals. The familiar inequality expressions given in elementary organic textbooks may help serve as a reminder for a few of the more common radicals . . .



However, these do not include all the radical forms that must be considered for the phenolic network. Also, the phenolic structure is strongly centered around aromatic functionality, not aliphatic character. Generally, the more carbon atoms there are surrounding the lone electron, the more stable the radical, and the greater the electron density near the lone electron, the lower the stability of the radical. When electron spin is allowed to delocalize across the molecule (via resonance or conjugation), the more stable the radical becomes.

There are many handbooks and databases available which provide a multitude of theoretical and experimental values for bond strengths as well as enthalpies of formation for a variety of free radicals and molecular pre-cursors. Also, in more recent years, many researchers have determined the energies for a large number of relevant compounds. Unfortunately, most of these bond energy values pertain to smaller molecules, not oligomers or polymer fragments. They are not very representative of the same bond types in larger molecules. This is due to localized conformational stresses and tertiary/quarternary effects within macromolecules and strained polymer segments that are not present in smaller molecules. However, since this type of data is the only indication of bond strengths readily available, we will make the best possible use of it for comparing and ranking the relative bond dissociation energies present in the cured phenolic resin structure. A closer examination of the structure suggested in Figure 1 would be convenient here. A post-cured version of that configuration is provided in Figure 8 below (note, post-curing will remove almost, if not all, of the ether links in the initially cured structure). Let us consider the various radicals that might form during thermal cleavage of some of the most important links in the phenolic network.

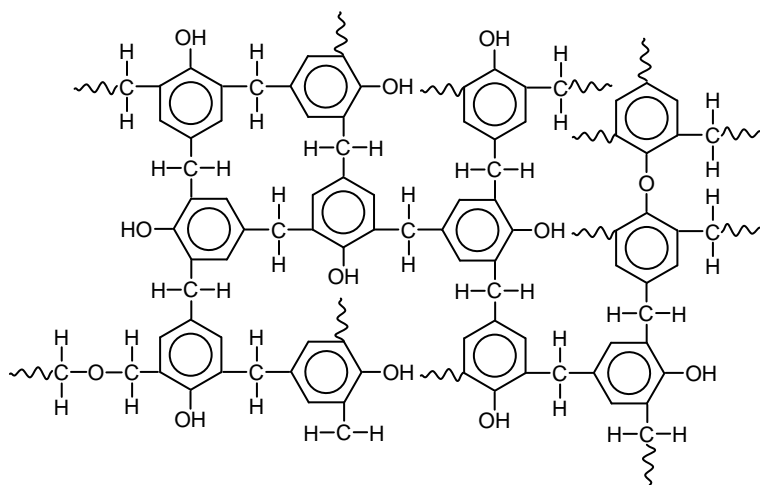
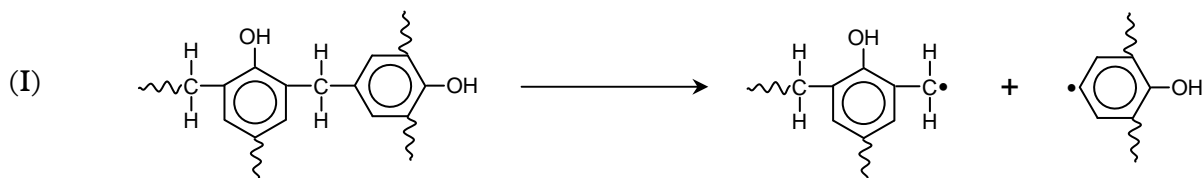


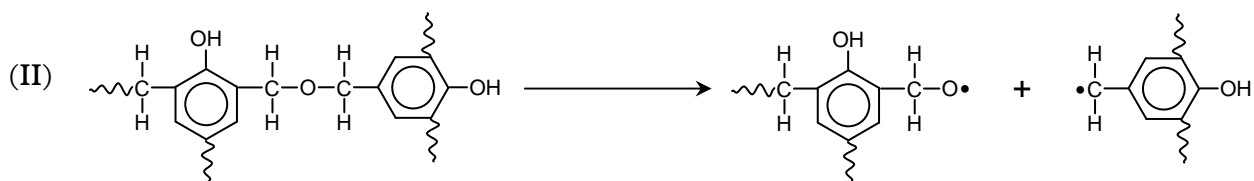
Figure 8. Suggested representation of an idealized cured phenolic resin structure.

» Cleavage of a methylene link to form a benzyl radical and a phenyl radical . . .



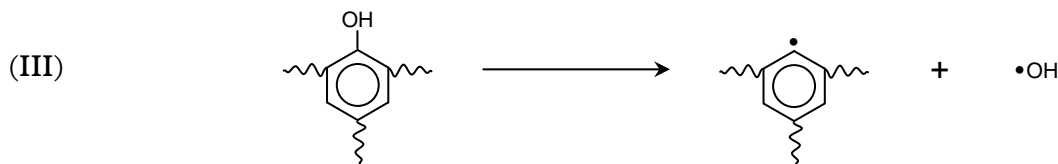
While benzyl radicals are known to be very stable, phenyl radicals are not as much so. The bond dissociation enthalpy for the same methylene link in diphenyl methane,  $Ph-CH_2-Ph$  has been determined by a number of workers<sup>[9][10][11]</sup>: 405.8, 333.0, 343.1, 348.9, 354.8, 374.9 and 367.4 kJ/mol with an average of 361 kJ/mol. Now the  $-OH$  groups and methylene links at all the ortho and para positions will enhance delocalization of the radical electron, so rather than use the average, we choose the lowest of the numbers and presume (just for our study) that the bond dissociation energy for the methylene link is approximately equal to 333 kJ/mol. Also, as we shall see, both of these radicals undergo rearrangements to produce even more stable radicals as pyrolysis/combustion commences.

» Cleavage of a methoxy link to form a benzyoxy radical and a benzyl radical . . .



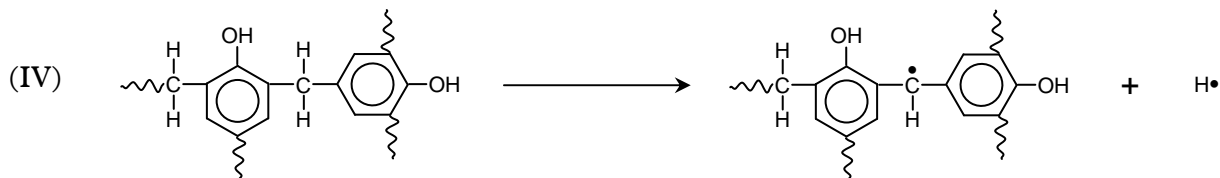
Both of these radicals are highly stable and the presence of methylene links on the benzyoxy radical enhances the radical even further. The bond strength of this link is expected to be relatively low. The only dissociation energy data that could be obtained with any similarity to this structure was the Handbook value for the methyl-benzyoxy link<sup>[12]</sup>  $CH_3-O-Ph$ , which is given as 280.3 kJ/mol. The occasional phenoxy-to-phenyl link that forms in the structure  $Ph-O-Ph$ , can also be considered to rupture at or before this level of energy is reached

» Cleavage of a hydroxyl link to form a phenyl radical and a hydroxy radical . . .



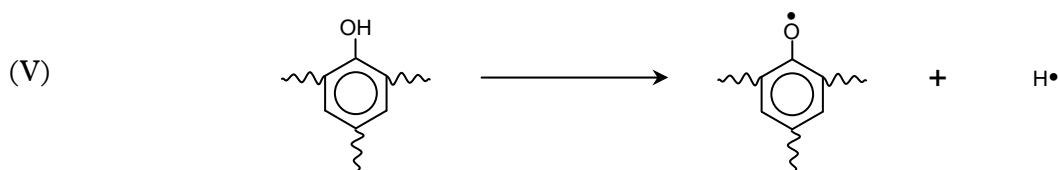
The bond dissociation enthalpy for simple phenol has been documented at 470.3 kJ/mol<sup>[9]</sup>. Given the resonance stabilization associated with these structures, this value should probably be notably lower, but for brevity, 470 kJ/mol is assumed (for this study) to represent the energy required to abstract an -OH group from the phenolic structure.

» Cleavage of a methylene hydrogen to form a diphenyl methyl radical . . .



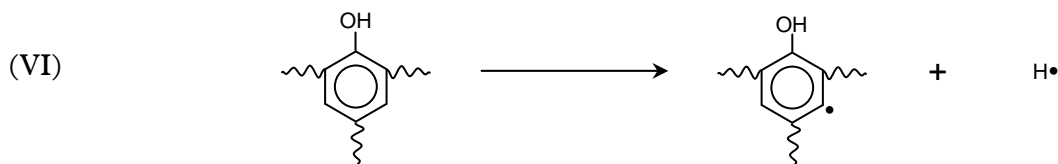
Here, the polymer backbone is not actually ruptured but at some point, stripping of hydrogens in the network must be considered. Recall that the ease of abstraction of hydrogen atoms follows the same priority as that for free radical formation. Thus, the benzylic hydrogen should be relatively easy to abstract. The methylene carbon-to-hydrogen bond energy for diphenyl methane has been experimentally determined and estimated<sup>[13]</sup>, 340.6 and 334.1 kJ/mol respectively. Again, due to the unusual stability with this configuration (relative to diphenyl methane), 334 kJ/mol is momentarily taken as the strength for this bond.

» Cleavage of a hydroxyl hydrogen to form a phenoxy radical . . .



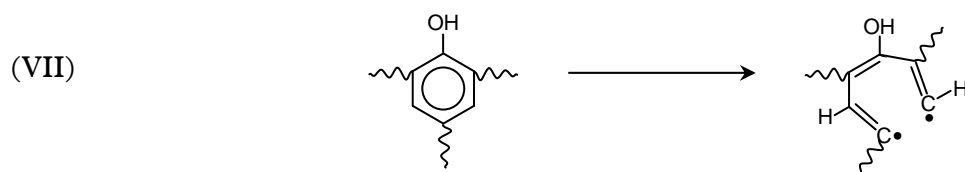
Like benzyl radicals, phenoxy radicals are low in energy as a result of electron delocalization and the availability of several resonating structures. Its bond strength is expected to be relatively low. For simple phenol, the bond dissociation enthalpy for the phenoxy-to-hydrogen link has been determined many times by several researchers<sup>[9][10][14]</sup>. The average of all these values is 365.3 kJ/mol with a minimum of 331.8 and maximum of 401.7 kJ/mol. For this study, its value will be taken as 331 kJ/mol.

» Cleavage of primary phenyl hydrogens to form phenyl radicals . . .



A number of authors have determined the bond dissociation energy for abstraction of hydrogen from the benzene ring<sup>[9][10][15]</sup>. The average of all these values is 476.0 kJ/mol with a maximum of 474 and a minimum of 463 kJ/mol.

» Cleavage of an aromatic ring to produce a linear diradical . . .



Cleavage of the basic phenyl structure is a ring opening process. The segment momentarily maintains conjugation, but becomes aliphatic as aromaticity is lost. While this bond strength is often estimated from aliphatic counterparts, there is no way to actually measure the aromatic resonance energy. One textbook source was identified and stated the measured the carbon-carbon net bond energy for simple benzene to be 518 kJ/mol<sup>[16]</sup> while the Handbook value gave 488 kJ/mol<sup>[12]</sup>. The average of these two is 503 kJ/mol.

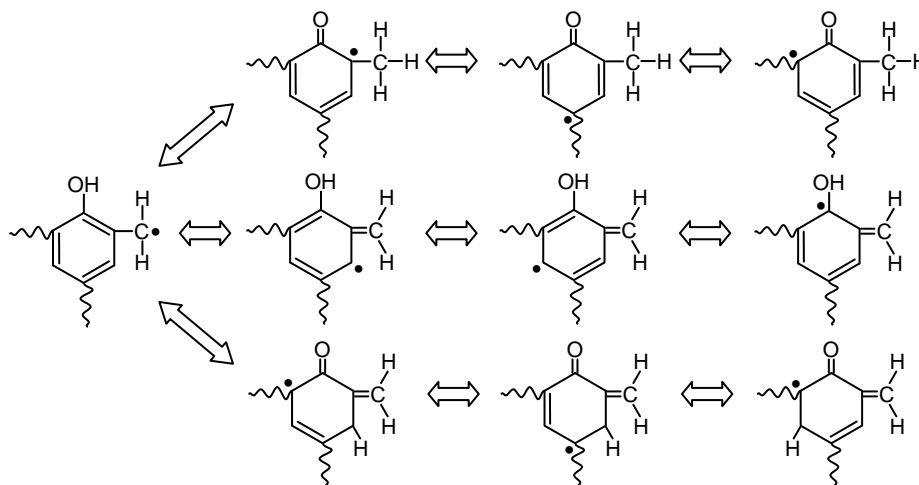
While there are surely other bonds that must be broken as the structure decomposes, these 6 or 7 reactions are relevant possibilities to consider during the initial and intermediate phases of the degradation process. Table 4 gives a summary and ranking of these results for comparative purposes.

Table 4 . Simplified ranking of relevant bond dissociation energies for the phenolic network.

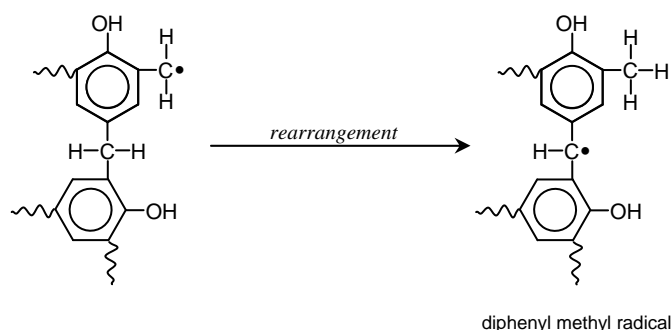
Bond/Link Description	Formula	kJ/mol
benzyl-benzoxy (ether) link	$C_6H_5CH_2 - OCH_2C_6H_5$	280
hydrogen-phenoxy link	$H - OC_6H_5$	331
phenyl-methylenel link	$C_6H_5 - CH_2C_6H_5$	333
hydrogen-methylene link	$C_6H_5 H - CH C_6H_5$	334
hydrogen-benzene link	$H - C_6H_5$	463
hydroxy-phenyl link	$OH - C_6H_5$	470
carbon=carbon benzene link	$\sim CH_2 = CH_2 \sim$	503

It should be emphasized that this over-simplified approach does not necessarily mean the links will rupture in the order given. On the contrary, one scenario might call for phenyl rings to remain intact throughout much of the pyrolysis cycle, in which case the associated phenyl hydrogens are not stripped off until late in the process - just before the aromatic carbons are converted into inorganic char. The primary benefit of this ranking exercise was to establish an apparent priority or guideline for bond scission and most importantly, to gain some insight as to which bonds might go first, i.e. . . . the 'weakest links'.

During the early stages of the decomposition process, Eq (I) becomes a very important reaction to take into account. It is suggested here that cleavage of the methylene link forms the basis for the initiation of phenolic matrix degradation. The ease of formation for the radicals generated in this step (and hence, the likelihood of Eq (I) occurring) can be supported by considering some of the resonance structures (equivalent rearrangements) available to these molecular fragments. Consider the possible resonance forms for the benzyl (or phenyl methyl) radical given in Eq (I) . . .

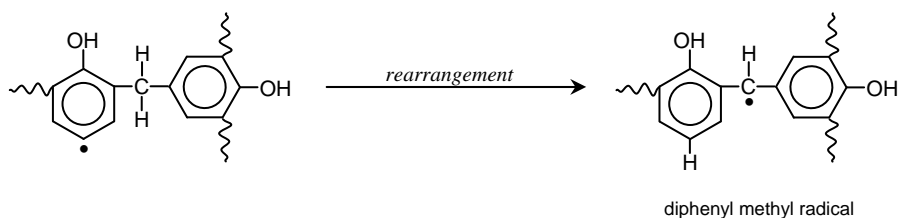


With so many available configurations to accommodate (delocalize) the radical electron here, it is not difficult to see why this radical has a high probability to form. However, consider the likely rearrangement that surely occurs when the lone electron is shifted inward to form the even more stable diphenyl (or diphenyl methyl) radical . . .

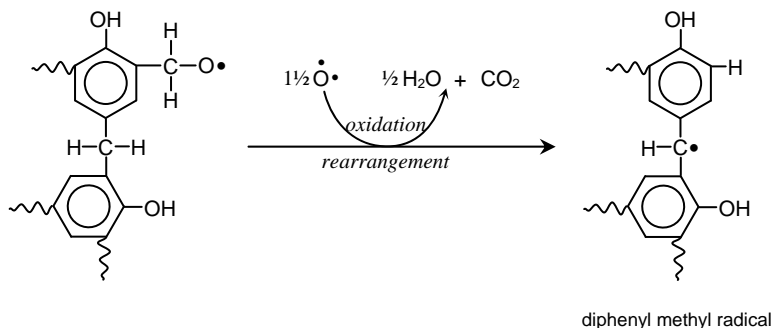


We shall not attempt to draw all the possible rearrangements for the diphenyl methyl radical here. Suffice it to say that, compared to the phenyl methyl radical, the number of resonance structures for this configuration is vast considering the fact that the lone electron now has at least two rings to spread over. This diphenyl methyl radical bears substantial similarity to the famous triphenyl methyl radical which is one of the most stable (and long-lived) radicals ever to be discovered. Interactions between di- and tri-phenyl methyl radicals are significant during the carbonization process and will be treated shortly. For the present however, it is suggested here that this species, *the diphenylmethyl radical may be the primary propagating radical in the decomposition of phenolic networks.*

Look again at Eq (I). The not-so-stable phenyl radical has an opportunity to rearrange itself . . .



Consider Eq (II) in which a benzoxy radical is generated. In the presence of a little oxygen (early in the decomposition process), rearrangement might bring about the following reaction in which  $\text{CO}_2$  and water are produced . . .



Where  $\dot{\text{O}}$  represents an oxygen atom or radical (oxygen is considered to be dissociated before entering the reaction process). It is suggested here that, for relatively slow heating rates ( $< 500^\circ\text{C}/\text{min}$ ) oxidation/combustion reactions tend to dominate the first portion of the overall degradation process and trickle off as pyrolytic reactions begin to take over. Using similar approaches, one can validate that reactions (III) through (VI) also lead (predominantly) to formation of the diphenyl radical with side reactions producing the components for water.

Although ring cleavage via Eq (VII) is believed to be a player in the decomposition process, complete destruction of the aromatic structure would produce a mixture of aliphatics. According to Table 2, methane was the only aliphatic compound detected, and this tends to indicate that: (1) phenyl rings are not generally disintegrated since this would likely lead to the formation, at least in trace amounts, of ethane, ethylene, propylene, etc..., and (2) methylene links are degraded, at least to a degree reflective of the fractional amount given in Table 2, which is relatively significant.

It is contended here that one of the primary reaction scenarios likely responsible for generating some of the observed gaseous products as well as char involves consolidation of neighboring phenyl rings, or ring fusion. Consider the following proposed pathways describing possible reactions involving the diphenylmethyl radical and leading to ring fusion under both pyrolytic (anaerobic) and oxidative conditions. First, pyrolysis of the diphenylmethyl radical is expected to give off methane and carbon monoxide, as well as form the precursor to char product, that is, fused ring segments . . .

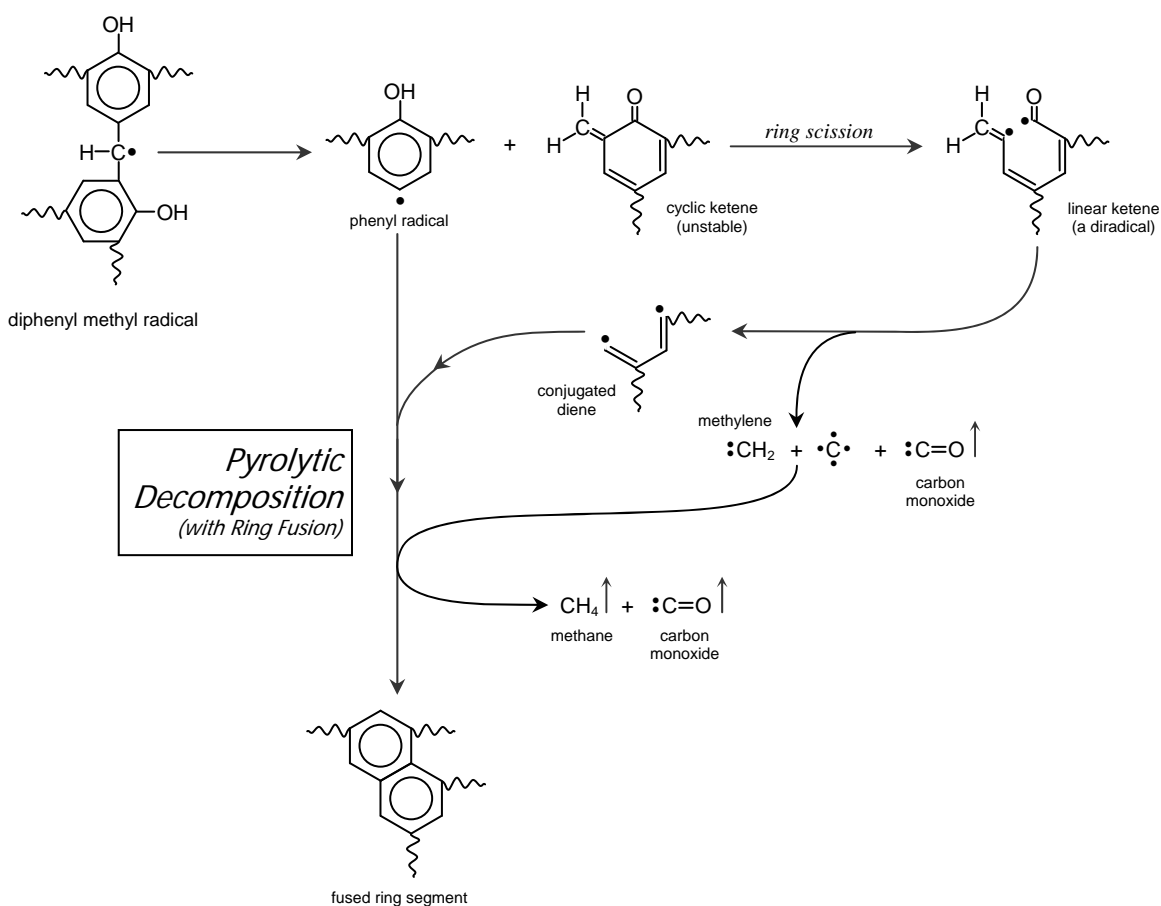


Figure 8. Schematic representation of a suggested pyrolytic reaction path that might take place during the formation of pyrolysis volatiles and char precursor based on consolidation or fusion of neighboring phenyl rings.

As heat is continually added to the system, the formation of less stable radicals becomes feasible. Here, the phenyl radical (step one) is presumed to survive long enough (without rearranging) to enter into the pyrolytic ring consolidation process illustrated in Figure 8. Formation of the unstable ketene intermediate leads to ring cleavage which results in the production of methane, carbon monoxide and sp<sup>2</sup> polynuclear aromatic domains.

Consider now an analogous scheme in which oxygen is locally available so combustion and partial oxidative reactions can take place. It is presumed that the process environment is conducive to molecular

bond scission so that oxygen (atomic) radicals are readily available as strong oxidizing agents. Now oxidation is more complex than pyrolysis since some products may be fully oxidized and others only partially oxidized. For instance . . .

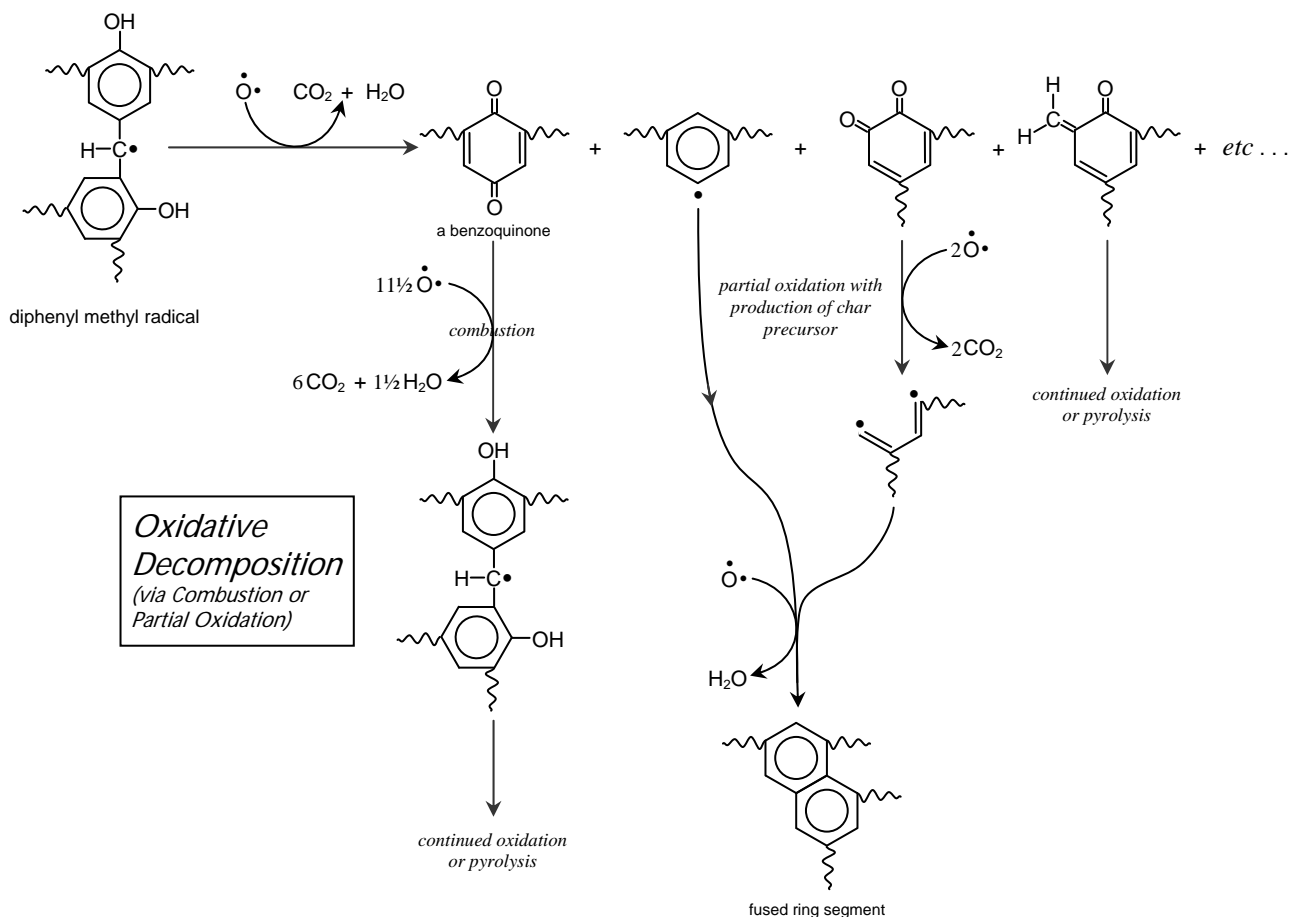


Figure 9. Schematic representation of a suggested oxidation and combustion reactions that might occur leading to the generation of pyrolysis volatiles and oxidation products with the possible formation of char precursor .

Continuation of the first reaction (oxidation of the quinone) would produce smaller and smaller fragments as the substrate underwent combustion. Note that certain reactions involving oxidation can lead to char production. This series of reactions illustrates the point that it is sometimes difficult to tell the difference between partial oxidation and pyrolysis. In general, oxidation results in the formation of combustion products (CO<sub>2</sub> and water) while pyrolysis generates CO, hydrocarbons and char. Aggressive or full oxidation should disintegrate most of the char formed in the process. Both pyrolytic and oxidative decomposition make use of Eq (VII).

Now if the fusion of phenyl rings was the only or even primary mechanism leading to char formation, the system would probably pass through mesophase and then graphitize. Also, if ring fusion within any given fragment is too extensive, then mesophase formation becomes possible. We know this does not occur. Ring consolidations within fragments that remain highly networked with aliphatic (methylene) crosslinks should not pass through mesophase. As a matter of fact, it has been revealed many times by direct experience that the production of glassy, non-graphitic char from cured phenolic resin is exclusively a solid state process – the formation of liquid or semi-liquid components has never been observed. Processes leading to ring fusion can only be considered as secondary pathways to solid state char production. On the other hand, a complete breakdown of the entire methylene link network would be contrary to the confirmed structure of phenolic-based glassy carbon substrates which are known to

retain a substantial resemblance to the original organic crosslinked polymer network, just as other glassy chars have been shown to resemble their specific precursors.

One of the most important phases of the decomposition process involves the removal or abstraction of hydrogen from the network. Due to the relative bond energies, dehydrogenation is expected to extract the aliphatic (methylene) hydrogen atoms before affecting the aromatic rings. Consider another reaction involving the diphenylmethyl radical . . .

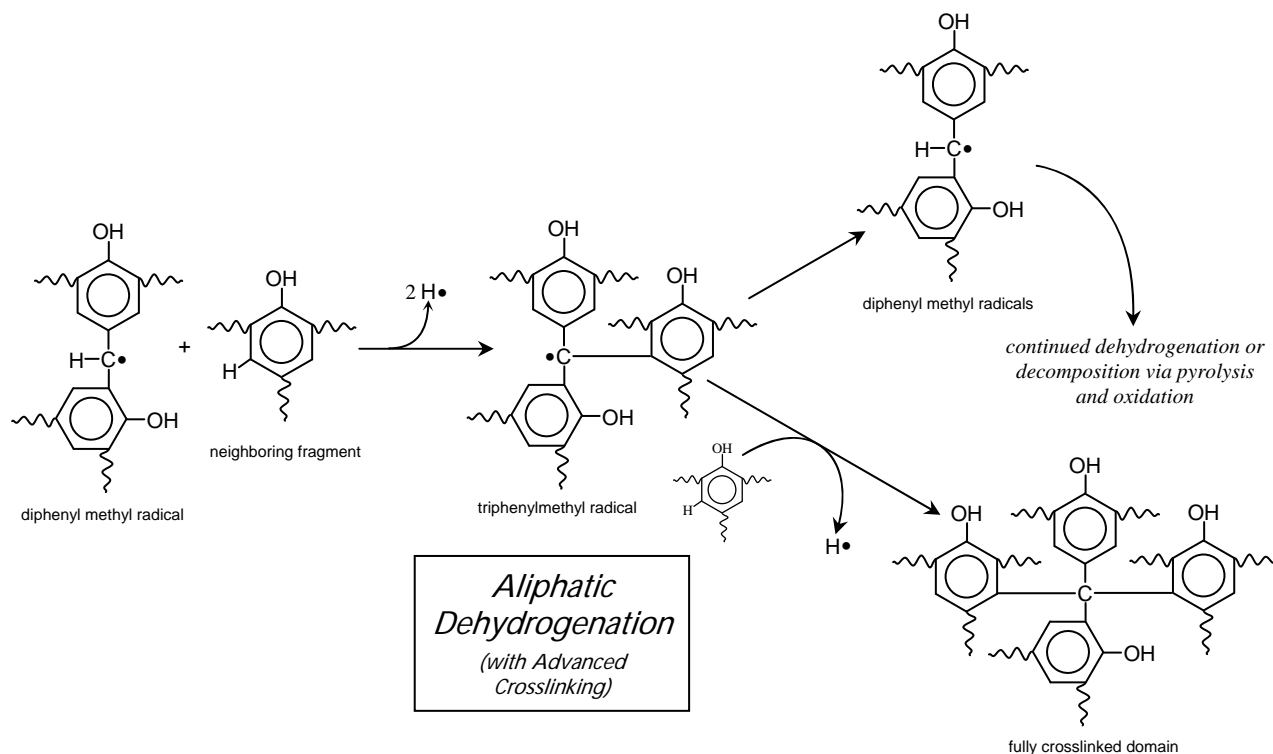


Figure 10. Schematic representation of suggested crosslinking reactions that most likely occur during the formation of rigid carbonized phenolic char in competition with and/or complimentary to ring consolidation reactions.

This scheme is an extension of Eq (IV). Here, it is entirely possible that the appearance of the diphenylmethyl *di*-radical is an intermediary to production of the triphenylmethyl radical. Formation of the extremely stable triphenylmethyl radical is very likely and affords the opportunity to either develop advanced crosslinks with available sites on neighboring phenyl rings or continue along pathways of pyrolysis/oxidation similar to those outlined in Figures 8 and 9. It is also obvious that neighboring di- and tri-methyl substituted phenyl rings will strongly direct ortho/para substitution during crosslink formation (that is, ortho/para relative to the methylene groups). The aliphatic hydrogen atoms generated here can combine and flow out of the system (to the GC detector for instance) or they may interact with other reactions taking place in the network (such as erosion). The additional crosslinks established in this part of the process are believed to enhance the already rigid crosslinked network that is reflective of the original organic phase. Obviously, formation of these links will be governed by steric hindrance factors and the local availability of phenyl reaction sites to methylene carbons (since all four methylene bonds become equivalently 'saturated', after this point, it may be more appropriate to consider them as methyl groups). It is believed that a majority of saturated aliphatic crosslinks are established before the higher energy aromatic hydrogens are affected.

While crosslinking contributes little, if any, to volumetric shrinkage of the substrate, it is believed that the majority of contraction comes about as a result of (1) ring consolidation or fusion, (2) erosion of

polymer end groups resulting in the release of low molecular weight organic compounds, and (3) abstraction of hydrogen (dehydrogenation). Examples of reactions responsible for generating pyrolysis gases, including pyrolytic methane and CO, as well as the major oxidation products CO<sub>2</sub> and water, have already been outlined, and are believed to contribute to the observed substrate weight losses occurring during the decomposition process. In addition however, it is suggested that bond rupture and degradation of peripheral polymer groups begins to occur releasing various amounts of benzene and phenol along with various fractions of their methyl derivatives. It is suspected that these compounds are due to pyrolytic (anaerobic) scission reactions which result in de-linking and partial stripping of terminal rings located near polymer ends across and within the surfaces of substrate fragments. Hydrogen atoms (radicals) present in the system from crosslinking reactions may facilitate this etching/degradation process. Making use of Eq (I), a simplified illustration might be suggested . . .

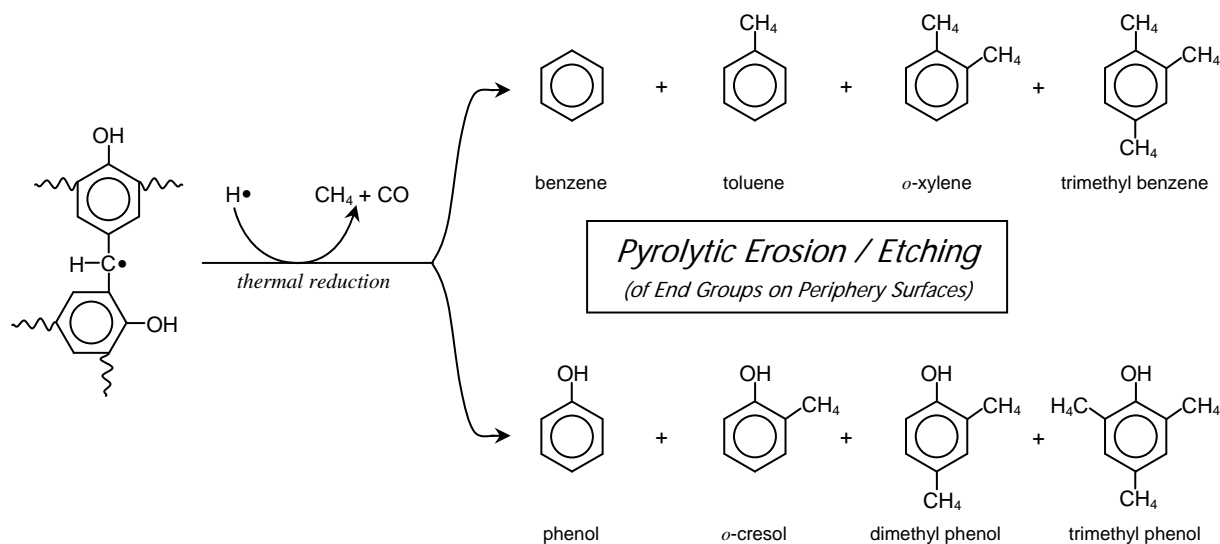


Figure 11. Schematic representation of suggested thermal erosion reactions that could be responsible for generating some of the organic gases released during the decomposition process.

The time-temperature regime where the reactions generating benzene derivatives occur appears to coincide approximately with and essentially overlap those reactions resulting in phenol and its derivatives (Table 2). The slight difference in release temperatures between the aryl rings and phenol rings may be due to residual hydrogen bonding effects between phenol groups. In both cases, it is suggested that these erosion reactions, take place predominantly across the open peripheral surfaces, internal pore surfaces, pore edges, openings, cracks and crevices resulting in general contraction (or volume loss) of the substrate accompanied by overall pore enlargement. This process can be defined appropriately as a form of pyrolytic etching or thermochemical erosion and is believed to be one of the primary pathways contributing to substrate weight loss during pyrolytic heating cycles and TGA tests.

Under ordinary (room) conditions, abstraction of hydroxy groups from the phenol ring is quite difficult. However, due to the elevated and increasing temperatures, production of less stable radicals is feasible and higher energy reactions become likely. Another reaction which must occur and contributes to substrate weight loss as well as volumetric contraction and production of CO is the abstraction and destruction of phenol hydroxy groups. Available methylene links and carbon radicals generated from other processes can facilitate the dehydroxylation reaction. A simplified version of the reaction might be illustrated by . . .

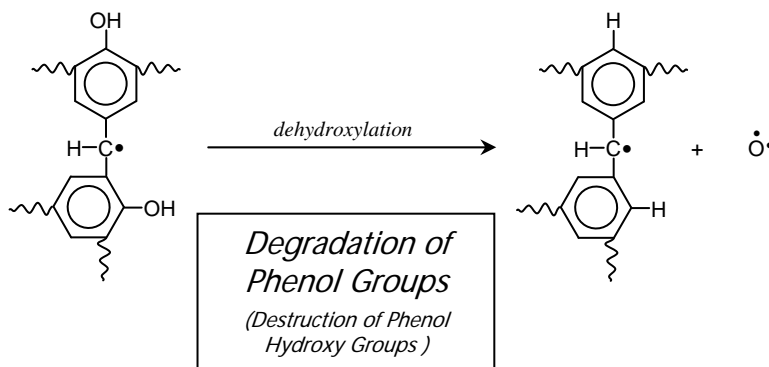


Figure 12. Possible scheme showing likely reaction for removal and disintegration of residual phenol hydroxy groups.

This is an extension of Eq (III). Considering the vast number of phenol rings present in the original system, the effects of this reaction could be relatively substantial. Oxygen radicals generated here can (1) initiate or enhance oxidative degradation (Figure 9), and/or (2) steal carbon atoms from pyrolytic degradation reactions and produce CO (Figure 8).

Now let us attempt to account for and rank the contributing processes and associated gases responsible for substrate weight loss during the decomposition of phenolic resin . . .

- (1) Pyrolytic etching/erosion of polymer end groups to produce methane, CO and aromatic derivatives.
- (2) Dehydrogenation of aliphatic and aromatic hydrogens to form molecular hydrogen.
- (3) Pyrolytic decomposition via ring cleavage with the release of methane and CO.
- (4) Oxidative degradation via ring destruction (combustion) generating CO<sub>2</sub> and water.
- (5) Abstraction and destruction of residual phenol hydroxy groups to produce reactive oxygen.

Obviously, the relative ranking of (3) and (4) is dependent on the level of available oxygen sources in the system. One may speculate on the fate of all these gases immediately after their production. Obviously, pyrolysis gases generated along surfaces are easily carried out of the system, almost instantly. However, gas molecules formed in the interior of the substrate must diffuse out of the confines of the micro-structure, rather rapidly. The full ramifications for rapid mass transport of these interior gases out of the system is not completely understood. It is suggested that diffusion of all the gaseous species generated throughout the decomposition process creates a sub-network of micro-porosity which interconnects with the larger pore channels to facilitate their removal.

Now it is presumed here that the methylene (or methyl) crosslinked network is essentially established before abstraction of aromatic hydrogens really takes off. In general, dehydrogenation begins sometime after the commencement of oxidation and ring fusion reactions and slowly increases as degradation progresses. Aromatic dehydrogenation comprises the last portion of the decomposition process with abstraction reactions becoming most aggressive up to the point of carbonization. As hydrogen is abstracted, carbonization (phase conversion) of the substrate progresses. Regions across the

network transform from the organic phase into inorganic carbon as localized domains of inert char begin to develop and expand. When hydrogen atoms are stripped off from a given molecular segment, all other reactions stop and that segment becomes fixed in space as hard, inorganic carbon. Abstraction of hydrogen marks the transition point from the reactive organic phase to the inert carbon state. From a simplified perspective, the carbonized structure might be visualized as randomly spaced regions or groups of 6 membered  $sp^2$  bonded cyclic structures held tightly within a network of  $sp^3$  crosslinks which prevent structural movement or mesophase formation. A simplified illustration of the carbonized structure might be represented by . . .

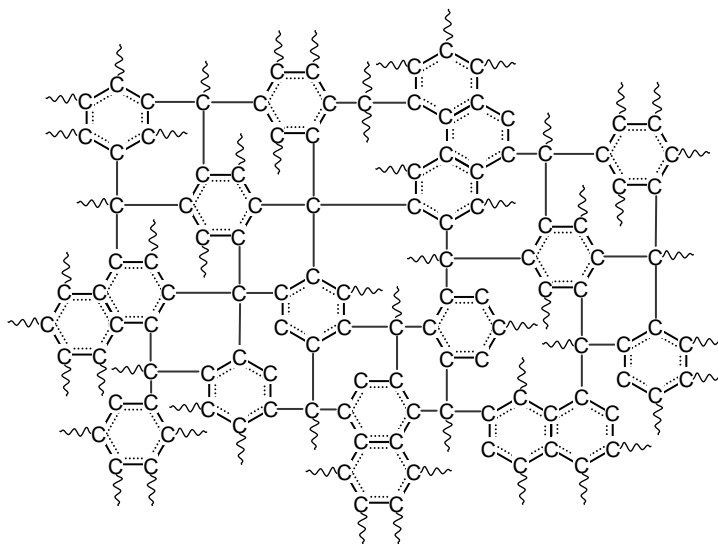


Figure 12. Schematic representation of suggested structure for fully carbonized phenolic resin showing pseudo-hexagonal ring sub-structures embedded within highly crosslinked glassy network.

Here, fully and partially saturated methylene links rigidly suspend a post-aromatic phase consisting of carbon residues of formerly substituted phenol rings and consolidated phenyl rings to form the overall inorganic structure. From a macro-structure perspective, the material would probably be considered as highly isotropic, monolithic and completely amorphous. From a micro-structure perspective, the material is probably anisotropic and multilithic with widely scattered domains of semi-crystalline nature. The chemical structure appears to accommodate both  $sp^2$  bonding (within the hexagonal cyclic groups) and  $sp^3$  bond orbitals (former methylene crosslinks). It would not be too surprising for the solid char to actually exhibit a bit of paramagnetism due to the possible existence of an intermittent free radical phase.

In light of the our discussion, we can now modify the classical free radical inequality and make the following claim pertaining specifically to radicals within the degrading phenolic network . . .

$$\text{Stability of Free Radical} = \text{Ease of Formation} =$$

$$\text{triphenylmethyl} > \text{diphenylmethyl} > \text{benzyl} > \text{phenoxy} > \text{alkyl} > \text{phenyl}$$

Thus, in conclusion, it is proposed here that the process of thermal decomposition of cured phenolic resin subjected to modest testing or firing conditions proceeds through a series of reactions and processes leading to both simultaneous and independent production of solid state char and pyrolysis gases as outlined in the following statements.

- (1) Random scissions along the methylene crosslink network (or backbone) which evolve into pyrolytic or oxidative pathways representative of those outlined in Figures 8 and 9 with the simultaneous production of char and pyrolysis / combustion gases, CO, CO<sub>2</sub>, methane and water.

- (2) Advanced crosslinking between methylene groups and available sites on neighboring phenyl rings brought about by aliphatic dehydrogenation which produces hydrogen and rigid interconnections within and between fragments as represented by the scenario given in Figure 10.
- (3) Pyrolytic erosion/etching of substrate surfaces, including pores and edges, cracks and crevices with the independent production of monomeric-type compounds reflective of the substrate's organic phase according to the representation given in Figure 11.
- (4) Abstraction and destruction of residual phenolic hydroxy groups on phenol rings. Liberated oxygen can promote continued oxidative degradation and/or retard pyrolytic ring consolidation. A potential reaction scheme is given in Figure 12, as well as Figures 9 and 10.
- (5) Abstraction of hydrogen from phenyl rings (aromatic dehydrogenation) causing phase conversion from aromatic organic carbon to inorganic carbon with the production of hydrogen. The level of unoccupied ring sites still holding hydrogen at this point is unknown. This completes the formation of char and the process of carbonization.

It can now be recognized that contributions to substrate weight loss come both from reactions that produce char with gases and reactions that produce only gases. In addition, it is suggested that variable and significant overlaps occur between these five phases of the process even though the indicated sequence is generally followed, on the average. Also, depending on the conditions of carbonization (maximum temperature, heating rate, environment), there inevitably will be some regions that do not undergo all the reactions and decomposition steps, perhaps due to shielding, and these areas may retain some of the original organic character. Final compositions for phenolic char, after heating to zero weight loss, have been reported<sup>[4][17]</sup>. Many of these results indicate that trace quantities of both hydrogen and oxygen are often present in the final char.

This initial paper is dedicated primarily to a survey and treatment of phenolic resins in order to help lay the ground work for future studies of CCP (Carbon Cloth Phenolic) nozzle composites. First, chemical aspects of the phenol-formaldehyde reaction and subsequent polymerization/crosslinking process are briefly covered. An awareness of some of the pathways associated with phenolic resin synthesis and production is helpful in understanding the ramifications and benefits carried over into the composite fabrication stage and subsequent carbonization process. Resols seem to make better carbonizing resins since they are known to contain fewer ether (oxygen) links and more methylene (carbon) crosslinks than their novolac counterparts. In addition to residual moisture, latent oxygen-bearing crosslinks are likely degradation points for early out-gassing episodes that subsequently lead to adverse effects in later operations or field use (such as delaminations).

Most amorphous forms of carbon are known to pass through a semi-liquid mesophase state (tar) in the 750-950°F range, re-structure into graphene (basal) planes later on and then begin to form graphite-like structures above 4000°F. Thermoplastic materials, which have a distinct melting point and glass transition temperature ( $T_g$ ) will readily form graphitizable, amorphous carbons. This pertains essentially to all linear (non-crosslinked) polymers. In many cases, these materials are treated via low temperature surface oxidation to convert their structures in to non-meltable graphite precursors in order to preclude formation of the mesophase state. On the other hand, most crosslinked polymers (thermosets) as well as many cyclic structures, are directly converted into a non-graphitizable glassy carbon without passing through mesophase. Non-graphitizable glassy carbon precursors would include the phenolic resins, epoxies, polyesters, etc... Other non-graphitizable hard carbon precursors include the cyclic structures of rayon and polyacrylonitrile (PAN). However, their carbonized forms are believed to contain at least limited amounts of 2-D graphitic-like planes, some of which may be capable of forming of 3-D crystallites or 'graphite-like' segments when exposed to high enough temperatures.

Degradation of phenolic networks necessarily includes (1) oxidation (partial), (2) combustion (full oxidation), and (3) inert pyrolysis, regardless of the firing conditions. In many instances and locations, the reactions associated with these processes are occurring simultaneously while there may also be a general sequence or progress the overall decomposition process follows as well. The major oxidation and pyrolysis phases appear to overlap substantially with oxidation playing a major role during the early portions of the degradation process, which gradually shifts into pyrolytic decomposition. A proper understanding of the phenolic carbonization process must include both oxidation and pyrolysis as primary degradation mechanisms occurring both concurrently and sequentially and in both inert and reactive environments.

Thermal decomposition of phenolic polymers (and most polymers for that matter) is dominated by the production of long-lived free radicals or better yet, multiple radicalized sites throughout the polymer substrate. The activities of these free radicals are suggested as the primary chemical entities responsible for the kinetics of decomposition. For this first paper, a simplified analytical approach describing the decomposition kinetics is developed and applied using data gathered from previous Thermogravimetric (TGA) tests on phenolic resin resols. This particular TGA data indicates three apparent phases across the degradation range in which oxidation/pyrolysis gases are released and then the Arrhenius kinetic parameters are estimated for each phase. Analytical data presented from studies published by other authors provides a semi-quantitative review of the primary TGA gaseous species generated at progressive temperatures across the decomposition range. This information may then used as a springboard to derive likely chemical mechanisms for char formation via phenolic decomposition into gases during subsequent sections.

A survey of bond dissociation enthalpies provides a guideline to further examine likely radicals formed during the phenolic degradation sequence and some of the rearrangements that occur. Initiation and propagation of phenolic decomposition is built around the premise that the most stable radicals form first and drive the carbonization process however, as the temperature inevitably increases, less stable radicals become available which account for many of the decomposition products generated. All indications are that the diphenyl methyl radical is the primary propagating intermediate (reactant) responsible for driving the various reactions throughout each of the decomposition phases. Pyrolytic decomposition is one the carbonization pathways leading to char through the process of benzene ring consolidation with the production of carbon monoxide. While oxidative degradation can lead to some ring fusion, its primary products are those of combustion that is, carbon dioxide and water. Abstraction of aliphatic hydrogen induces advanced crosslinking within the network via formation of the triphenyl methyl radical, big brother to the diphenyl methyl radical. Pyrolytic chemical erosion or etching of polymer ends along substrate surfaces, in cracks, crevices, pore surfaces and openings is believed to be one of the primary pathways leading to the formation of observed methane, benzene/phenol and its derivatives. Destruction of phenol hydroxy groups (dehydroxylation) is expected to contribute to weight loss and latent oxidation of the network and may possibly exhibit a slight pyrolysis inhibitor effect. Abstraction and removal of aromatic hydrogen from the system marks the transition point from the reactive organic phase to the inert carbon state. Overall, the system of reactions that makes up the total decomposition process includes reactions that produce both char and gases, reactions that produce char only and those that only form gases. Thus, the decomposition scenario proposed here seems to account for all the gases detected, produces an abundant amount of char and supports findings by other workers which indicate the possible presence of both crystalline-like structure ( $sp^2$  bonding) and amorphous character ( $sp^3$  bonding). It is suggested that the inorganic macro-structure is comprised of hexagonal rings (which may exhibit some sort of inherent resonance) suspended or fixed within a rigid amorphous-like network. This is the basic description of the unusual carbon form referred to as glassy or vitreous carbon which is the solid reaction product of carbonized phenolic resin.

While there are a number of important issues and uncertainties to be resolved in the near future, only a few are mentioned here as possible topics for further investigation. Several more should be added as time goes on. The following descriptions, comments and recommendations are presented in an informal fashion, in no special order and most are not intended to provide comprehensive answers but to raise awareness of some of the concerns in an inquisitive approach, and in some cases, demonstrate possible benefits of a particular approach. Comments and conclusions are solely the author's perception.

- (1) Heating rate anomalies: Kinetic studies conducted by Eric Stokes on MX4926 NARC material in the 1990's revealed an unusual effect associated with TGA heating rates<sup>[5]</sup>. In this study, a number of independent TGA samples were subjected to a spread of heating rates from 3°C/min all the way to 1000°C/min. The averages of those results are shown in Figure 13 which gives the first TG derivative for the decomposition region for each heating rate studied.

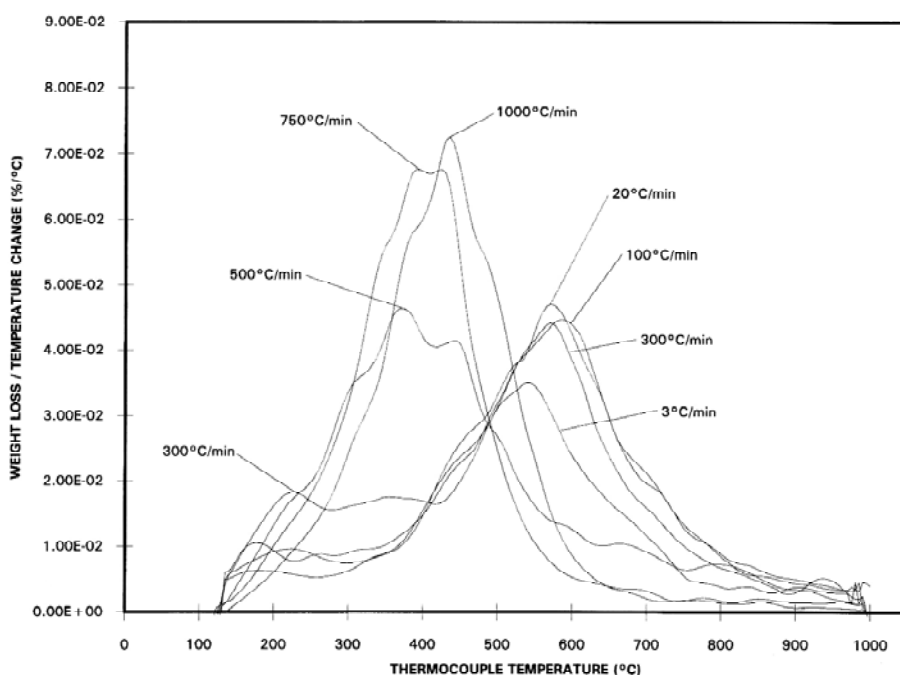


Figure 13. Mean Weight Corrected Average Derivative TG Curves as a Function of Heating Rate.

Somewhere in between the 300°C/min heating rate and 500°C/min, the decomposition process changes with respect to the weight loss indicated. The exact phenomena taking place here is not well understood yet but future studies will focus on possible causes that may play a role in this effect. One thing seems apparent however. At some point after 300°C/min, the major pyrolytic degradation reactions that normally occur during the higher temperature regimes, appear now to completely overlap the earlier oxidation processes taking place during the first phase of the cycle. Further examinations into the properties associated with heating rate are recommended in order to better understand the specific mechanisms and kinetics associated with extremely rapid carbonization. Also, at the higher heating rates, it is possible that additional oxidation reactions may result in a slight reduction in char yield as reported by Eric for heating rates in excess of 300°C/min.

- (3) An interesting short table of data presented in Thoeni, Baker and Smith's paper (discussed earlier)<sup>[8]</sup> included measured values of carbon content at the various temperatures studied for urethane-furfurylol polymer foam. These values have been plotted and best fitted to a response-type exponential functions as shown in Figure 14. Functions of this sort are not unusual when exploring carbon conversion processes dealing with organic precursors. A better understanding of this analytical approach can often prove beneficial for material systems undergoing quasi and rapid carbonization processes.

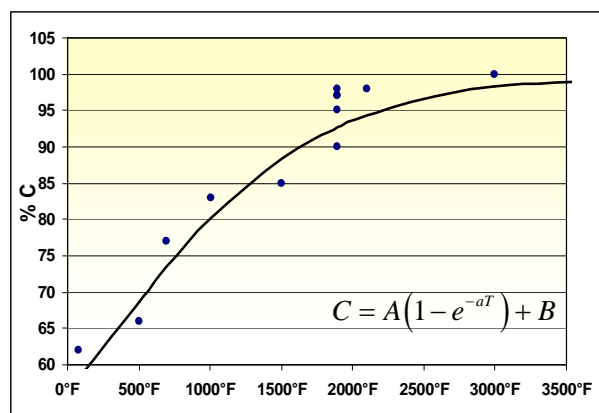


Figure 14. Carbon weight fraction change as a function of process temperature for urethane-furfurylol polymer foam.

- (4) Benefits of post curing: It cannot be over-emphasized, all phenolic-based materials that are expected to see elevated field temperatures should be post-cured to preclude subsequent potential failures and catastrophic defects. History has repeatedly proven that post curing of phenolic systems will minimise pore pressure build-up, subsequent delaminations and will beneficially modify the matrix Tg so that it is closer to the carbonization/conversion phase and becomes more obscured thus reducing its tendency to mobilize. However, in conjunction with the initial autoclave cure, the post-cure process must be applied correctly, and this is where many companies attempting to evaluate its effects run into problems. Typical post cure time/temperature profiles consist of multiple steps over 5 to 7 days that take the part up to the 450°-500°F regime so that residual volatiles and stresses are eased out or gradually released without creating addition stresses or deleterious pore pressure effects (which might occur during a rapid post-cure).

Additionally, parts should de-bagged and not re-bagged, they should not be left on their original tooling or sealed up in any way, they should be de-tooled and simply placed in an air-circulating oven with minimal restraints to maintain part tolerances; the post-cure configuration must not retard the free release of residual volatiles during the baking process. There is strong historical evidence indicating that the phenolic polymerization/curing or crosslinking process is a *temperature-driven* process while the nature and formation of porosity, voids and interconnecting tunnels within the phenolic network are influence most significantly by the *time at temperature*. In other words, the production of cure reaction moisture occurs predominantly as a result of the temperature that the system is subjected to (as opposed to length of time it is held there) while the interconnectivity, pore diameter and ultimate contiguity of the resulting matrix porosity is controlled by the length of time the system remains in the gelled and post-gelled (early hardening) states. Thus, the initial autoclave cure (time/temperature profile) must compliment the post-cure. Excessively long autoclave cure profiles will tend to close off the interconnecting porosity network within the phenolic matrix long after the bulk of the crosslinking reactions have occurred, trapping current and subsequent condensation moisture within the matrix porosity. Residual water in phenolics is not desirable. In addition to the trapped moisture fraction, a substantial portion of the residual moisture will be comprised of reaction sites that have not yet formed crosslinks (ie... uncured material). The actions and consequences of this condition are straightforward – one can either drive out the residual moisture during the fabrication process . . . or run the risk of anomalous substrate problems later on when the water molecules are catastrophically forced out. This is a choice that we (the designer/fabricator) get to make.

- (5) Theories based on 'the impermeable char cap' <sup>[18][19]</sup>: If the char cap is truly impervious causing catastrophic pore pressure build-up, what specific mechanisms are responsible? Future objectives should include studies to help characterize the role of the matrix during this process and any possible contributions the fiber phase and carbon black may have.
- (6) Liquid pyrolysis products: Eric Stokes has routinely reported the formation of pyrolysis liquids (tar) in CCP materials when test samples reached pyrolysis temperatures ( $\sim 880^{\circ}\text{F}$ )<sup>[18]</sup>. The contention has been that these liquid products clog up pores and cracks preventing adequate ventilation of pyrolysis gases. Since these observations have been noted at heating rates of  $3^{\circ}\text{C}/\text{min}$ , it is obvious this liquid material is not due to rapid heating effects. A strong possibility would be the formation of carbon black mesophase. It is conceivable that higher MW phenolic erosion products could form, but experience teaches that phenolic polymers undergo conversion into glassy carbon entirely in the solid state with no liquids (or tar) formed.

On the other hand, the amorphous carbon black powder which is incorporated into the composite substrate (at  $\sim 15\%$  levels) is known to pass through mesophase in the  $800^{\circ}\text{-}950^{\circ}\text{F}$  range. Experience teaches that carbon black is not readily dispersible in most polymer solutions. As a matter of fact, hundreds of surfactants and dispersing agents have been personally tested in attempts to successfully disperse or suspend this fluffy black powder within liquid resin binders. The particles always agglomerate within seconds (this may be due to electrostatic charges on the particle surfaces). In a composite network, they will tend to migrate and attach to themselves, rather than associating with resin molecules or fiber surfaces. It would not be surprising to discover that carbon black mesophase is clogging up pore exits and cracks in CCP materials. Tests to confirm this effect might be recommended as well as composite panel fabrication trials evaluating its reduction in the formulation (at least below its percolation threshold which probably runs between  $\sim 4\text{-}7\%$ ) . . . or possibly . . . its complete removal altogether from the prepreg resin formulation. There is strong evidence that powdered fillers are not needed in CCP composites to facilitate resin shrinkage, conductivity, pore filling or any other conceived notion.

- (7) Physical property testing: Substrate porosity and true resin content (resin weight fraction) are critical properties that need to be measured diligently. Variations in either of these components from panel to panel can spell disaster if not monitored closely. Also, it is inevitable that significant variations in total porosity and resin content exist from region to region within any given panel. These variations are established by the specific molding process (as well as the part configuration), and there is no doubt that geographical trends in their values can be used to facilitate improvements in the fabrication process. Nitric acid digestion is the standard and most reliable method for determining resin content in carbon fiber composites. From a chemist's point of view, it is a fairly simple test to run, as long as the composite consists only of digestible resin and inert fiber. Other components can complicate the procedure. At the present, SRI may be the best source for generating this data since they have already developed a seemingly accurate procedure, but development of a robust in-house technique would be recommended.

It might be noted here that *permeability does not equal porosity*. The total porosity of any composite is simply the sum of the open (or pervious) porosity and the closed (or impervious) porosity. Unfortunately, the closed porosity comprises an unknown fraction of the total porosity and obviously, methods need to be refined to estimate its value since this is where most of the 'pore pressure' likely develops. Permeability is based on the hydraulic gradient established along the sample length or thickness. For a given dimension, permeability would be a subset of the open porosity (however, in composites and ceramics, the perception is that most 'open' pores are only accessible from one

opening). He picnometry may be the best method for determination of total porosity. Open (apparent) porosity measurements can also easily and quickly be accomplished (in house) by a simple water penetration or impregnation test. Based on Archimedes principle, this test will provide fairly accurate values for apparent porosity (% open porosity volume fraction), the corresponding apparent density (composite bulk density) and the true composite density (impervious density). Bulk densities measured by water penetration and geometrically measured densities should be identical, but they are not always. The Archimedes densities are more consistent, and when needed for special applications, they correspond exactly with their measured porosities. At least two techniques of this sort have been personally developed and applied over a thousand times on a variety of porous materials, particularly fibrous composites. It is a proven method for quick and accurate determination of composite open porosity (and bulk density). Also, mercury porosimetry is unacceptable for composite materials since it destroys the very property under study . . . been there, done that.

Resin flow, viscosity, degree of cure, cure volatiles, residual volatiles, resin solids and char yield are all properties associated exclusively with the resin phase and cannot be accurately ascertain without neat samples of resin for characterization. Obscure, third party information for these parameters should not be acceptable. Most of this data should be documented and readily available from both the resin manufacturer and the prepregger. Otherwise, the capabilities exist in-house to accomplish many of these tests, and since the resin is the primary phase undergoing change during the carbonization process, the need to characterize the resin by itself is justified. There is already ample historical data and information available for such tests performed on full CCP composites and prepreg samples. However, tests performed at this level may not always tell the complete story regarding issues and effects that are resin-controlled. Perhaps it is time to dig a little deeper.

- (8) Kinetics of carbonization: Expansion and improvement of Eq (2) and the theory developed in that section should be pursued. From Table 1, it seems likely that  $E_{a,subA}$  pertains heavily to the initial oxidation/combustion reactions taking place (Figure 9), while  $E_{a,subB}$ , if it actually exists, could imply an increase in pyrolytic ring fusion (Figure 8), and  $E_{a,subC}$  may be a conglomerate of dehydrogenation, dehydroxylation, pyrolytic erosion and ring consolidation. While there is a slight concern as to the validity of this approach for estimating the pre-exponential kinetic parameters, it may be possible to obtain some other benefits from the results. Additional information regarding overlap of the three sub regions shown in Figures 5, 6 and 7 would be interesting. Overlap between the reactions occurring in sub regions A, B and C is substantial but the exact degree of overlap is unknown. Let us prepare for integration and re-write Eq (1) in terms of the degree of conversion  $\alpha$  (weight fraction of material that has been converted into product relative to reactant) . . .

$$-\frac{d\alpha}{dT} = \frac{k}{\beta}(1-\alpha)^n$$

$$-\int \frac{d\alpha}{(1-\alpha)} = \frac{A}{\beta} \int e^{-E_a/RT} dT \quad (5)$$

Evaluation of the integral on the right side is not straightforward. The method used to resolve this integral is given in the Appendix. Keeping in mind that it is only an approximation and may only be valid over a limited temperature range, the degree of conversion within one of the sub-regions can be roughly estimated by . . .

$$\alpha \approx 1 - \exp \left[ -\frac{AR}{\beta E_a} \left( 1 - 2 \frac{RT}{E_a} \right) e^{-E_a/RT} T^2 \right] \quad (6)$$

Using the estimated kinetic parameters from Table 1 and Eq (6), relative values for the extent of conversion for each sub region across the decomposition temperature range can be computed and compared as shown in Table 5. Figure 15 gives a plot of this data which illustrates the exponential nature of these reactions.

Table 5. Estimated relative values for degree of conversion for each sub-region across the entire decomposition range.

	533K 500°F	600K 621°F	631K 676°F	655K 720°F	719K 835°F	730K 855°F	750K 891°F	763K 915°F	781K 946°F	812K 1002°F	850K 1071°F	890K 1143°F	911K 1180°F	977K 1299°F
Sub Region A	0.001	0.005	0.012	0.022	0.096	0.121	0.179	0.231	0.319	0.543	1.000	-----	-----	-----
Sub Region B	0.005	0.034	0.073	0.127	0.461	0.563	0.799	1.000	-----	-----	-----	-----	-----	-----
Sub Region C	0.000	0.000	0.001	0.002	0.016	0.021	0.035	0.049	0.074	0.148	0.328	0.692	1.000	-----

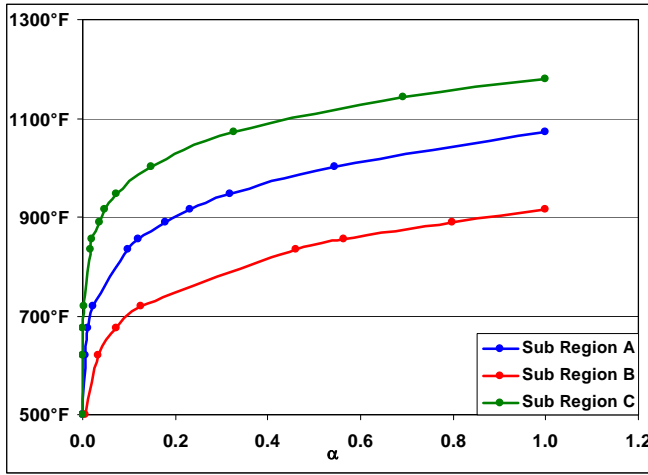


Figure 15. Plots of estimated degree of conversion for the three sub-regions across the temperature range.

If this data tells a valid story, reactions in sub-region A are still occurring well into sub-region C. As one might expect, reactions in sub-region C are parallel to and indeed are a part of the processes going on in sub-region A. The conversion process is essentially complete at about 1200°F. There is little doubt that the matrix is the primary phase under attack during the decomposition process. Other than the carbon black component, which passes through mesophase somewhere during the 800°-950°F regime, the matrix (phenolic resin transforming into vitreous carbon) is still the primary component undergoing change. Any uncarbonized or partially

converted fiber regions within the reinforcement phase should not begin to react until well above 1500°-1800°F.

In a series of previous studies investigating pyrolytic conversion of CCP-type materials into carbon-carbon<sup>[20]</sup>, an original system of expressions was developed to help monitor changes in composite physical properties from one carbonized state to the next. Adaptation of these tools may provide some interesting benefits when applied directly to the carbonization process itself (that is, the carbonization transition state). Consider the basic composite statement relating the bulk density  $\rho_B$  to the fiber volume fraction  $f_V$ , its corresponding density  $\rho_f$ , the matrix volume fraction  $m_V$  (fraction of resin and/or carbonized resin), and its density  $\rho_m$ , ...

$$\rho_B = f_V \rho_f + m_V \rho_m$$

Now since  $f_w + m_w = 1$  (where  $f_w$  and  $m_w$  are the corresponding weight fractions),  $f_V + m_V + p = 1$  (where  $p$  is the total porosity fraction), and volume fractions are related to their weight fractions via their corresponding densities,  $f_V = f_w \rho_B \rho_f^{-1}$  and  $m_V = m_w \rho_B \rho_m^{-1}$ , then the basic statement can be written with inclusion of the total composite porosity ...

$$\rho_B = (f_w \rho_f^{-1} + m_w \rho_m^{-1})^{-1} (1 - p)$$

If the carbon black component  $b_w$  is included (as it is in exit cone CCP panels), rearrangement gives an expression for the composite porosity ...

$$p = 1 - (f_w \rho_f^{-1} + m_w \rho_m^{-1} + b_w \rho_b^{-1}) \rho_B \quad (7)$$

In future studies, it may be helpful to further develop these tools in order to explore the physical changes occurring to CCP substrate specifically during the short transition period it is undergoing carbonization. For the moment however, and for the sake of brevity, let us neglect the carbon black component and presume that the matrix fraction is the only component undergoing change during the carbonization process. This implies that the matrix density, composite bulk density and fiber weight fraction are also change accordingly. In this scenario, as heat is carbonizing the matrix, the porosity volume fraction is also changing that is, it is increasing. The temperature derivative of the porosity in Eq (7) may give a clue. During the transition state . . .

$$\begin{aligned} \frac{dp}{dT} &= f_w \rho_f^{-1} \frac{\partial \rho_B}{\partial T} + \rho_B \rho_f^{-1} \frac{\partial f_w}{\partial T} + m_w \rho_m^{-1} \frac{\partial \rho_B}{\partial T} + \rho_B \rho_m^{-1} \frac{\partial m_w}{\partial T} + m_w \rho_B \frac{\partial \rho_m^{-1}}{\partial T} \\ &= m_w \rho_B \rho_m^{-2} \frac{\partial \rho_m}{\partial T} - \left[ \frac{\partial \rho_B}{\partial T} (f_w \rho_f^{-1} + m_w \rho_m^{-1}) + \rho_B \rho_f^{-1} \frac{\partial f_w}{\partial T} + \rho_B \rho_m^{-1} \frac{\partial m_w}{\partial T} \right] \end{aligned}$$

A quick check of this approach would require some before and after values for the material system under investigation. Since there is currently not enough relevant data available for the CCP RSRM composite platform, let us use some values determined in a previous study examining PAN-based RCC-type composites which were converted from autoclave cured CCP into the first carbon-carbon state. First, the measured apparent porosity for this study gave  $p_0 = 4.3\%$  in the as-molded composite (after autoclave cure) which became  $p_1 = 22.3\%$  after carbonization to 1500°F over several hours. This gives a change in the apparent porosity of  $\Delta p = 18.0\%$  due to pyrolytic conversion of the composite to the first carbon state. The measured (geometrical) bulk density of the as-molded composite and then its bulk density after carbonization were respectively,  $\rho_{B0} = 1.59 \text{ g/cm}^3$  and  $\rho_{B1} = 1.40 \text{ g/cm}^3$ . The as-molded resin content (or as-cured matrix weight fraction) was determined to be  $m_{w0} = 26.0\%$  which dropped to  $m_{w1} = 16.4\%$  after carbonization (estimated using Eq (8)). The corresponding fiber weight fractions are then  $f_{w0} = 74.0\%$  and  $f_{w1} = 83.5\%$  respectively. The apparent density of the particular fiber used in this composite platform had been documented by the vendor (and by in-house measurements) to be  $\rho_f = 1.91 \text{ g/cm}^3$ . Now the apparent densities of cured phenolic resin and carbonized phenolic resin (same as SC-1008) have already been personally determined many times to be  $\rho_{m0} = 1.24 \text{ g/cm}^3$  and  $\rho_{m1} = 1.43 \text{ g/cm}^3$  respectively. Plugging these numbers into the formula above gives a porosity change (increase) of  $\Delta p = 20.8\%$  after complete conversion which, when compared to the measured values, may indicate a small but significant level of impervious or closed porosity generated during the carbonization process.

In lieu of actual transition state data, for this quick example, let us use a functional form which has repeatedly shown relevance to properties undergoing pyrolytic conversion processes, analogous to that given in Figure 14. Presumably, the apparent porosity at any time during the firing/carbonization process can be given as a function of temperature, such as . . .

$$p = A(1 - e^{-cT}) + p_0$$

Now resolution of the heating rate,  $\beta = dT/dt$  gives  $T = (\beta t^2 + 298)^{1/2}$ , but for simplicity and brevity at this time, let's just write . . .

$$p = A(1 - e^{-kt}) + p_0$$

(More detailed and elaborate analysis are saved for future studies; the current supplemental discussion is just a quick survey to demonstrate the tools, approaches and possibilities.) Now the behavior of the apparent porosity according to this function is illustrated in Figure 16 where the porosity asymptotes its limiting value over the firing time (or temperature).

Whatever the actual functional form is during the firing process, it has been repeatedly shown in the pyrolysis of RCC-type materials that changes in most of the inter-related physical properties tend to parallel each other functionally, including some of the mechanical attributes, such as flexural and interlaminar tensile strength.

Ultimately, our quest is to determine the appropriate functional descriptions for the critical CCP composite properties that define its behavior during the nozzle liner carbonization process. Experience teaches that a thorough understanding of the behavior and properties of each of the components, as individual contributors, is mandatory in order to adequately comprehend the behavior and properties of the full composite form.

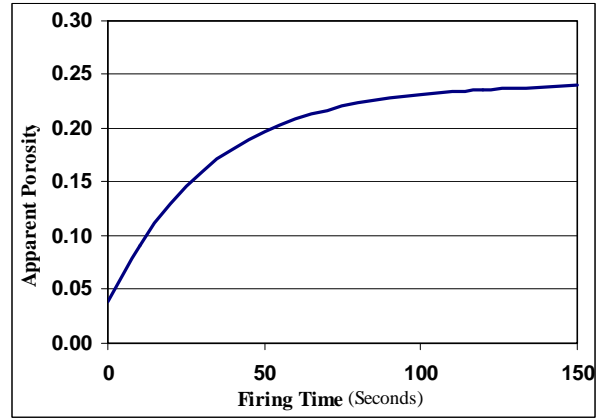


Figure 16. Possible behavior of porosity as a composite is subjected to a given heating rate over time.

Now the char yield of cured phenolic resin samples pyrolyzed to 1500°F over several hours has been measured numerous times with an average of  $y = 56.0\% = w_{m1} / w_{m0}$  where  $w_{m0}$  is the weight of matrix in a composite, a TGA test or a small resin sample before carbonization, and  $w_{m1}$  is the matrix weight carbonization. When a composite panel with an as-molded (post autoclave) weight of  $w_0$  undergoes carbonization, its weight decreases to  $w_1$  so the weight loss upon carbonization is given by  $\eta = (w_0 - w_1) / w_0$  or  $w_1 = w_0 (1 - \eta)$ . If the matrix is treated as the only component changing, then . . .

$$\eta = \Delta m_w = m_{w0} (y - 1)$$

where  $m_{w0}$  is simply the measured as-molded resin content value. If  $w_f$  is the unchanging weight of fiber in the composite, then the matrix weight fraction after carbonization becomes . . .

$$\begin{aligned} m_{w1} &= 1 - \frac{w_f}{w_1} = 1 - \frac{w_f}{w_0 (1 + \eta)} = 1 - \frac{f_{w0}}{1 + \eta} \\ m_{w1} &= 1 - (1 - m_{w0}) (1 + \eta)^{-1} \\ m_{w1} &= 1 - (1 - m_{w0}) [1 + m_{w0} (y - 1)]^{-1} \end{aligned} \quad (8)$$

which gives the matrix content after carbonization in terms of the original resin content (weight fraction of carbonized phenolic resin in the composite). The author is unaware of any practical method to physically measure  $m_{w1}$ ; Eq (8) was specifically developed to estimated this quantity. Its result is dependent-free of any other component that might be present in the formulation. Now if we recognize the degree of matrix conversion going from organic polymer to inorganic char by noting that  $y = 1 - 0.44\alpha$ , then Eq (8) can be given as . . .

$$m_{w1} = 1 - (1 - m_{w0})(1 - 0.44m_{w0}\alpha)^{-1}$$

and during the transition state . . .

$$\frac{dm_w}{dT} = -0.44m_{w0}(1 - m_{w0})(1 - 0.44m_{w0}\alpha)^{-2} \frac{d\alpha}{dT}$$

which can be rearranged to give . . .

$$\frac{d\alpha}{dm_w} = k_1(1 - k_2\alpha)^2$$

When compared to Eq (5), this statement expresses the degree of resin carbonization relative to the change in composite matrix content. Does this result infer any information regarding the kinetics for carbonization of the composite substrate? That matter that will be taken up in future reports.

Before ending this section, consider a quick estimate, for example, of the as-molded total porosity and subsequent carbonized matrix content using data from the MX4926 NARC control panel given in ATK's Final Report for Screening of NSP Carbonized Rayon Replacement Materials from 2001<sup>[21]</sup>. While many properties were measured during this program, porosity was not, and since there is no way to even measure the carbonized matrix content, let us roughly estimate these quantities here using Eq (7) and Eq (8). Now the as-molded resin content was given as 34.7%; the average carbon black content, 15.5% (and using a density of 1.85 g/cm<sup>3</sup>); the measure fiber density was given as 1.85 g/cm<sup>3</sup> (with a corresponding fiber content of  $f_{w0} = 1 - m_{w0} - b_{w0}$ ); the as-molded bulk (geometrical) density average was 1.50 g/cm<sup>3</sup>; and of course the previously measured values for cured phenolic resin density, char density and yield are still valid. This gives an estimated as-molded total porosity for the NARC control panel in this study of  $p_0 = 5.1\%$  and a matrix content after carbonization of  $m_{w1} = 22.9\%$ .

Future segments of this task will further expand and apply some of the techniques introduce here directly into the CCP platform. Needless to say, a reliable knowledge of component parameters, properties and processing data can help carve the way to a solid understanding of the carbonization transition process in phenolic-based composites.

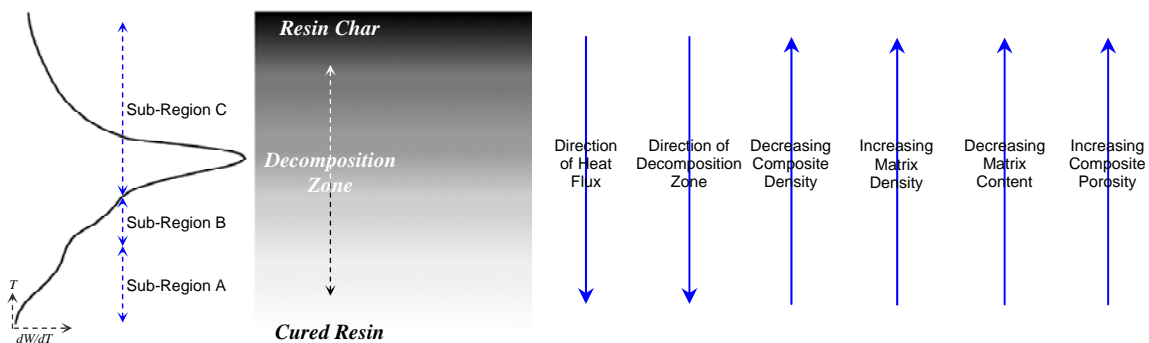


Figure 17. Simplified illustration showing some of the critical parameters relevant to the decomposition/carbonization zone during a slow heating rate.

## Appendix

Method for the evaluation of the integral . . .  $\frac{A}{\beta} \int e^{-E_a/RT} dT$

Let  $x = -\frac{E_a}{RT}$  so that  $dT = \frac{E_a}{Rx^2} dx$  then

$$\frac{A}{\beta} \int e^{-E_a/RT} dT = \frac{A E_a}{\beta R} \int x^{-2} e^x dx$$

Now this integral has already been evaluated and is given in the Handbook of Chemistry and Physics<sup>[12]</sup>:

$$\begin{aligned} \int x^m e^{ax} dx &= e^{ax} \sum_{r=0}^m (-1)^r \frac{m! x^{m-r}}{(m-r)! a^{r+1}} \\ &= \frac{e^{ax}}{a} \left( x^m - \frac{mx^{m-1}}{a} + \frac{m(m-1)x^{m-2}}{a^2} - \dots \right) \end{aligned}$$

Taking  $m = -2$ ,  $a = 1$ ,  $r = 0, -1, -2$  and using only the first two terms, the solution becomes . . .

$$\begin{aligned} \frac{A}{\beta} \int e^{-E_a/RT} dT &= \frac{A E_a}{\beta R} e^{-E_a/RT} \left( \frac{R}{E_a} T^2 - 2 \frac{R^2}{E_a^2} T^3 \right) \\ &= \frac{AR}{\beta E_a} \left( 1 - 2 \frac{RT}{E_a} \right) e^{-E_a/RT} T^2 \end{aligned}$$

## References and Information Sources

1. Textbook on Polymer Science, 3<sup>rd</sup> Ed., *Fred W. Billmeyer, Jr.*, John Wiley & Sons, 1984
2. "Analysis of Phenolic Resins for Carbon-Carbon", *Randy Lee*, LTV Aerospace & Defense Co., Space Shuttle LESS Program 1985
3. "New Perspectives on the Structure of Graphitic Carbons", *Peter J. Harris*, *Critical Reviews in Solid State and Materials Sciences*, 30:235-253, 2005.
4. "Characterization of Phenolic Resins with Thermogravimetry-Mass Spectrometry", *Cherng Chang, Juanita R. Tackett*, Energy Citations Database, 1990.
5. "Kinetics of Pyrolysis Mass Loss from MX4926 Standard Density NARC-Based Carbon Phenolic Composite", *Eric H. Stokes*, Southern Research Institute, 1994.
6. "Determination of Kinetic Parameters for the Thermal Decomposition of Phenolic Ablative Materials by a Multiple Heating Rate Method", *B. Henderson, M.R. Tant, and G.R. Moore*, *Thermochimica Acta*, 1981, 44, 253.
7. "Effect of Heating Rate on Thermal Decomposition Kinetics of Fiberglass Phenolic", *K. N. Ninan*, *Journal of Spacecraft and Rockets*.
8. "Preparation and Properties of Carbon Foam", *A.K. Thoeni, G.K. Baker, C.H. Smith*, *Journal of Cellular Plastics*, The Bendix Corporation, 1971.
9. Blanksby, S.J.; Ellison, G.B. *Acc.Chem. Res.* 2003, 36, 255.
10. van Scheppingen, W.; Dorrestijn, E.; Arends, I.; Mulder, P. J. *Phys. Chem. A* 1997, 101, 5404-5411.
11. Yao, X.-Q.; Hou, X.-J.; Wu, G.-S.; Xu, Y.-Y.; Xiang, H.-W.; Jiao, H.; Li, Y.-W, *Phys. Chem. A* 2002, 106, 7184-7189.
12. Handbook of Chemistry & Physics, CRC Press, 60<sup>th</sup> Edition
13. Cherkasov, A.; Jonsson, M.; *Chem. Inf. Comput.* 2000, 40, 1222-1226.
14. Laarhoven, L. J. J.; Mulder, P.; Wayner, D.D. *Acc. Chem. Res.* 1999, 32, 342-349.
15. Senosian, J. P.; Han, J. H.; Musgrave, C. B.; Golden, D.M. *Faraday Discuss.* 2001, 119, 173-189.
16. "Organic Chemistry", 6th Edition, *John McMurry*, 2003 (Brookes/Cole).
17. H. W. Lochte, E.L. Strauss, R. T. Conley, J. *Applied Polymer Science*, 9, 2799, 1965.
18. "In-Plane Gas Permeability of Enka and NARC based CCP as a Function of Across Ply Stress and Temperature", *Eric H. Stokes*, Southern Research Institute, March 2007.
19. "Ply Lifting Technical Interchange Meeting", Singer, Kay, Porter, Richardson, Heman, McCann, MSFC, January 2007.
20. "Relationships in Carbon-Carbon Processing, A Model for Advanced Composite Fabrication and Densification", *Randy Lee*, LTV Aerospace & Defense Co., Space Shuttle LESS Program, 1986.
21. "TWR-76249 Final Report For PTP-0417 Phase I. Screening and Down-Selection of Rayon Replacement Materials (NSP Carbonized Materials)", Rita Tellers, Aug. 17, 2001.